



Environment
Canada

Environnement
Canada

National Hydrology Research Institute

CAI
EP 501
- 1988
P35

3 1761 11552849 9



NHRI PAPER NO. 35

IWD SCIENTIFIC SERIES NO. 157



Physical Limnology of an Ice-Covered Lake with Through-Flow: Lake Laberge, Yukon Territory

E.C. Carmack, R.C. Wiegand, E.M. Marles, M.E. Alford and
V.A. Chamberlain

NHRI

INLAND WATERS/LANDS DIRECTORATE
NATIONAL HYDROLOGY RESEARCH INSTITUTE
NATIONAL HYDROLOGY RESEARCH CENTRE
SASKATOON, SASKATCHEWAN, 1987

(Disponible en français sur demande)



Environment
Canada

Environnement
Canada

CAI
EP501
-1988
P35

National Hydrology Research Institute

NHRI PAPER NO. 35 | IWD SCIENTIFIC SERIES NO. 157

Physical Limnology of an Ice-Covered Lake with Through-Flow: Lake Laberge, Yukon Territory

E.C. Carmack,* R.C. Wiegand,† E.M. Marles,‡ M.E. Alford§ and
V.A. Chamberlain||

E.C. Carmack, R.C. Wiegand, E.M. Marles, and V.A. Chamberlain prepared this paper while with the National Water Research Institute, Pacific and Yukon Region, West Vancouver, British Columbia; M.E. Alford was with the Water Survey of Canada, Water Resources Branch, Inland Waters Directorate, Pacific and Yukon Region, Whitehorse, Yukon Territories.

The authors are currently at the following addresses:

* E.C. Carmack Fisheries and Oceans Canada
 Institute of Ocean Sciences
 9860 West Saanich Road
 Sidney, British Columbia

† R.C. Wiegand SciTech Consultants Inc.
 1330 Fulton Avenue
 West Vancouver, British Columbia

‡ E.M. Marles Inland Waters/Lands Directorate
 National Hydrology Research Institute
 National Hydrology Research Centre
 Saskatoon, Saskatchewan

§ M.E. Alford Yukon Expeditions
 127 Alsek
 Whitehorse, Yukon Territory

|| V.A. Chamberlain Environmental Protection Service
 100 Park Royal
 West Vancouver, British Columbia

NHRI

INLAND WATERS/LANDS DIRECTORATE
NATIONAL HYDROLOGY RESEARCH INSTITUTE
NATIONAL HYDROLOGY RESEARCH CENTRE
SASKATOON, SASKATCHEWAN, 1987

(Disponible en français sur demande)

National Hydrology Research Institute

WATER PAPER NO. 36 / 1988

Physical Limnology of an Ice-Covered Lake with Thermal Stratification Lake Laberge, Yukon Territory

E. G. Carmack, R. C. Wiegand & E. W. Johnson
V. A. O'Brien

The physical limnology of Lake Laberge, a large, ice-covered lake in the Yukon Territory, is described. The lake is characterized by a long, narrow shape and a shallow depth. The physical limnology is characterized by a long, narrow shape and a shallow depth. The lake is characterized by a long, narrow shape and a shallow depth.

The physical limnology of Lake Laberge, a large, ice-covered lake in the Yukon Territory, is described.

The physical limnology of Lake Laberge, a large, ice-covered lake in the Yukon Territory, is described. The lake is characterized by a long, narrow shape and a shallow depth. The physical limnology is characterized by a long, narrow shape and a shallow depth.

The physical limnology of Lake Laberge, a large, ice-covered lake in the Yukon Territory, is described. The lake is characterized by a long, narrow shape and a shallow depth. The physical limnology is characterized by a long, narrow shape and a shallow depth.

The physical limnology of Lake Laberge, a large, ice-covered lake in the Yukon Territory, is described. The lake is characterized by a long, narrow shape and a shallow depth. The physical limnology is characterized by a long, narrow shape and a shallow depth.

The physical limnology of Lake Laberge, a large, ice-covered lake in the Yukon Territory, is described. The lake is characterized by a long, narrow shape and a shallow depth. The physical limnology is characterized by a long, narrow shape and a shallow depth.

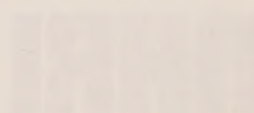
The physical limnology of Lake Laberge, a large, ice-covered lake in the Yukon Territory, is described. The lake is characterized by a long, narrow shape and a shallow depth. The physical limnology is characterized by a long, narrow shape and a shallow depth.

Published by authority of
the Minister of the Environment

© Minister of Supply and Services Canada 1988

Cat. No. En 36-502/157E

ISBN 0-662-15934-9



Contents

	Page
MANAGEMENT PERSPECTIVE	v
ABSTRACT	vi
RÉSUMÉ	vii
INTRODUCTION	1
LITERATURE REVIEW	2
STUDY AREA AND METHODS	5
ENVIRONMENTAL PARAMETERS	6
Hydrology	6
Ice and snow cover	7
Meteorology	9
WINTER TEMPERATURE STRUCTURE	10
Forcing parameters	10
Thermal history	10
Heat budget	11
THROUGH-FLOW AND WATER MASS FORMATION	12
Temperature and conductivity sections	12
Temperature and conductivity correlation diagrams	13
Horizontal property distributions	13
Inlet dynamics	14
Outlet dynamics	17
DISCUSSION	18
REFERENCES	18
APPENDIX A. Data from the 1982/83 pilot study	21
APPENDIX B. Meteorological data	25
APPENDIX C. Turbulent velocity scales.	29
APPENDIX D. Seasonal temperature structure	33
APPENDIX E. Temperature and conductivity sections	49
APPENDIX F. Horizontal property and distribution maps.	53

Illustrations

	Page
Figure 1. Yukon River basin	1
Figure 2. Schematic of YISEX	2
Figure 3. Lake Laberge bathymetry and station locations.	4
Figure 4. Area and volume as functions of depth	5
Figure 5. Streamflow of the Yukon River out of Lake Laberge	6
Figure 6. Water level of Lake Laberge.	6
Figure 7. Mean ice thickness at the Jackfish Bay section	7
Figure 8. Ice conditions at the inlet of Lake Laberge.	7
Figure 9. Ice conditions at the outlet of Lake Laberge.	8
Figure 10. Mean snow depth at the Jackfish Bay section	8
Figure 11. Snow depth in relation to equivalent snow mass at the Jackfish Bay section	8
Figure 12. Snow mass in relation to the deficit water level at the Jackfish Bay section	9
Figure 13. Incident solar radiation in relation to reflected solar radiation at the Jackfish Bay section	9
Figure 14. Solar radiation at the ice/water interface in relation to solar radiation 1 m below the ice/water interface at the Jackfish Bay section	9
Figure 15. Volume-weighted mean temperature as a function of time.	11
Figure 16. Heat flux as a function of time.	12
Figure 17. T/C_{25} correlation curves at three midlake stations for each of the three lakewide surveys and schematic diagram showing T/C_{25} curve evolution arising from through-flow.	14
Figure 18. Pro-deltaic channels in the inlet	15
Figure 19. Plots showing (a) study area for the inlet survey, (b) ice thickness and water depths, and (c) the horizontal profile of velocity at the inlet	16
Figure 20. Temperature near the inlet	16
Figure 21. Density gradient near the inlet.	16
Figure 22. Open water surface area at the outlet	17
Figure 23. Temperature section near the outlet	17

Management Perspective

Although lakes in the north spend more than six months of the year under a roof of ice, thermodynamics and hydrodynamic processes continue unabated year round. These processes largely determine the time frame over which lake ice can be used for winter roads and the nature and timing of ice breakup in spring. This natural limnological environment is also vitally important to birds, fish, and other nonhuman users of northern lakes. As interest in the north increases, the impact of lakes and ice on travel and development will increase. At the same time, pollution and other negative effects of human activity will begin to have an impact on the other users and on the lakes themselves.

This important report details the results of a study of a large northern lake with continuous winter through-flow, historic Lake Laberge. In addition to providing specific background data on winter limnology and the ice cycle in Lake Laberge, the study represents the first comprehensive treatment of the interaction of winter through-flow and lake circulation under ice in the north.

Chief
Limnological Research Division

Abstract

The objective of the Yukon Ice Seasonality Experiment (YISEX) is to obtain an understanding of physical processes affecting ice cover on northern lake and river systems. Towards this goal, limnological studies were carried out during the winters of 1982/83 and 1983/84 on Lake Laberge, a long (48 km), narrow (4.2 km), deep (mean depth = 54 m), medium residence-time ($T_r = 1.06$ a) lake in the Yukon Territory. A record is given here of the evolution of thermal structure, ice growth and decay, and the attendant meteorological and hydrological conditions.

During late summer and fall, circulation and mixing are forced by the wind and by surface heat exchange. At this time the surface heat flux is typically 175 to 200 W m^{-2} ; also wind-generated internal seiche amplitudes of up to 40 m are observed. In late autumn the lake becomes nearly isothermal at 4°C, and then enters inverse stratification.

Lake Laberge is frozen from late December to early June. Ice cover is characterized by rapid change during freeze-up and breakup, and by gradual change in midwinter. The midwinter equilibrium thickness is 0.8 to 1.0 m. Anomalous ice conditions exist at the inlet and outlet of the lake because of enhanced vertical mixing in these areas. Subsequent to ice cover formation, the wind and surface heat exchange become negligible, and river through-flow is the main source of turbulent mixing.

Spring warming of the lake begins in April with the breakup and warming of the upstream river and with the onset of radiation-driven convection. Heat continues to penetrate the lake as it nears breakup and spring overturn in early June.

Under-ice circulation patterns associated with the riverine circulation include entrance mixing, through-flow, and selective withdrawal at the outlet. The river enters the lake as a turbulent jet, thus entraining water from below and enhancing vertical heat transfer. Since the inflow has a temperature near 0°C, it spreads as a buoyant plume within the upper layers of the lake. T/C_{25} correlation diagrams show that the through-flow is confined to the upper 15 to 20 m of the lake. The flow is further influenced by Coriolis forces, so that the riverine flow is most intense along the eastern margin of the lake. The current is also acted on by frictional resistance, both at the ice/water interface and at lower levels, thus effecting an Ekman-type transport of water away from the eastern margin of the lake and broadening the current downlake. At the outlet of the lake, upwelling and increased flow velocities combine to support a large area of open water (outlet polynya) and thin ice.

The general requirements for one-dimensional modeling of ice-covered lakes include the proper parameterization of mixing processes and river-induced circulation, inclusion of the thermodynamic properties of fresh water, and allowance for variable wind, snow, and cooling conditions at freeze-up.

Résumé

L'objectif de l'Expérience de saisonnalité glacielle du Yukon (ESAGY) est d'expliquer les processus physiques qui influent sur le manteau glacielle dans les réseaux hydrographiques (lacs et cours d'eau) du Nord. À cette fin, des études limnologiques ont été effectuées durant les hivers 1982-1983 et 1983-1984 dans le lac Laberge, qui est un lac long (48 km), étroit (4.2 km), profond (54 m en moyenne) et à temps de séjour moyen ($T_r = 1.06$ a) du Yukon. Nous décrivons dans ce rapport l'évolution de la structure thermique, la croissance et la décroissance de la glace ainsi que les conditions météorologiques et hydrologiques associées.

À la fin de l'été et au cours de l'automne, la circulation et le mélange des eaux sont intensifiés par les vents et les échanges thermiques à la surface. Le flux thermique à la surface est alors de façon typique entre 175 et 200 $W\ m^{-2}$; en outre, des seiches internes dues au vent, dont l'amplitude peut atteindre 40 m, sont observées. À la fin de l'automne, le lac devient presque isotherme à 4 °C, et la stratification inverse commence.

Le lac Laberge est gelé de la fin de décembre au début de juin. Le manteau glacielle change rapidement pendant la prise des glaces et la débâcle, mais les changements sont graduels au milieu de l'hiver. L'épaisseur d'équilibre au milieu de l'hiver est de 0.8 à 1.0 m. À l'entrée et à la sortie du lac, les conditions de la glace ne sont pas normales en raison du mélange vertical qui y est plus intense. Après la formation de la couche de glace, l'influence du vent et des échanges thermiques à la surface devient négligeable, et le courant fluvial est la principale source de mélange par turbulence.

Le réchauffement printanier du lac commence en avril quand le cours d'eau en amont dégèle et se réchauffe et quand la convection due aux radiations commence à agir. Le lac continue de se réchauffer, puis surviennent la débâcle et le renversement printanier au début de juin.

La circulation fluviale sous la glace a certaines particularités, comme les propriétés de mélange à l'entrée, d'écoulement continu et de sélection à la sortie. Les eaux turbulentes de la rivière entrent dans le lac, entraînent l'eau des couches inférieures et favorisent un échange thermique vertical. Puisque ces eaux turbulentes sont à une température près de 0 °C, elles s'étalent comme un panache flottant dans les couches supérieures du lac. Des diagrammes de corrélation T/C_{25} indiquent que l'écoulement continu se limite à la zone de 15 à 20 m d'épaisseur située dans la partie supérieure du lac. Comme l'écoulement est également soumis aux forces de Coriolis, il est plus intense le long de la rive est du lac. L'écoulement de l'eau dépend aussi de la résistance au frottement, tant à l'interface glace-eau que dans les zones plus profondes. Ce phénomène affecte donc le transport d'eau, de type Ekman, au fur et à mesure qu'on s'éloigne de la rive est du lac. Ce phénomène crée aussi un élargissement de l'écoulement de l'eau dans la partie aval du lac. À la sortie du lac, les remontées d'eau et les vitesses accrues créent une large étendue d'eau libre (polynie) et de glace mince.

La modélisation unidimensionnelle des lacs couverts de glace entraîne les données suivantes: formulation appropriée des paramètres pour les processus de mélange et la circulation générée par les eaux fluviales; propriétés thermodynamiques de l'eau douce; facteurs de variation des conditions climatiques comme le vent, la neige et le refroidissement au moment de la prise des glaces.



Digitized by the Internet Archive
in 2022 with funding from
University of Toronto

<https://archive.org/details/31761115528499>

Physical Limnology of an Ice-Covered Lake with Through-Flow: Lake Laberge, Yukon Territory

E.C. Carmack, R.C. Wiegand, E.M. Marles, M.E. Alford and V.A. Chamberlain

INTRODUCTION

Lake Laberge is a long, deep lake that lies along the course of the Yukon River at approximately 61° N (Fig. 1). The lake is frozen from December to June.

Robert Service's poem "The Cremation of Sam McGee" gives a mystical image of winter on Lake Laberge.

There are strange things done in the midnight sun
By the men who toil for gold;
The Arctic trails have their secret tales
That would make your blood run cold;
The Northern Lights have seen queer sights,
But the queerest they ever did see
Was that night on the marge of Lake Laberge
I cremated Sam McGee.

This poem refers to the lake's use as a wintertime path to the Klondike gold fields. In truth, the lake did impose a number of difficulties on northern travelers. Because of its depth and great heat capacity, it froze over late, thus delaying winter travel. And while a thick, stable cover eventually developed on the lake, mixing at its inlet and outlet areas resulted in dangerous areas of thin ice and open water. Indeed, as related by Jack London in *The Call of the Wild*, the outflow reach of Lake Laberge, the so-called Thirty Mile River, was easily the most demanding part of the winter trail between Whitehorse and Dawson.

The Thirty Mile River was wide open. Its wild water defied the frost, and it was in the eddies only and in the quiet places that the ice held at all. Six days of exhausting toil were required to cover those thirty terrible miles. And terrible they were, for every foot of them was accomplished at the risk of life to dog and man. A dozen times, Perrault, nosing the way, broke through the ice bridges, being saved by the long pole he carried, which he so held that it fell each time across the hole made by his body. But a cold snap was on, the thermometer registering fifty below zero, and each time he broke through he was compelled for very life to build a fire and dry his garments.

With the onset of spring, the ice cover on Lake Laberge posed a different problem. Breakup of the river is usually complete by mid-May or earlier, but the ice cover on the lake remains until early June. Paddle-wheel operators, anxious for an open route, were inspired to devise ways to speed the date of ice out. For example, soot was spread over the lake's surface to increase the absorption of solar radiation, and a water storage structure was built at the outlet of Marsh Lake so that an impulse of water could be sent downriver to break the ice cover mechanically. Today, two dams are operated upstream from Lake Laberge, but not

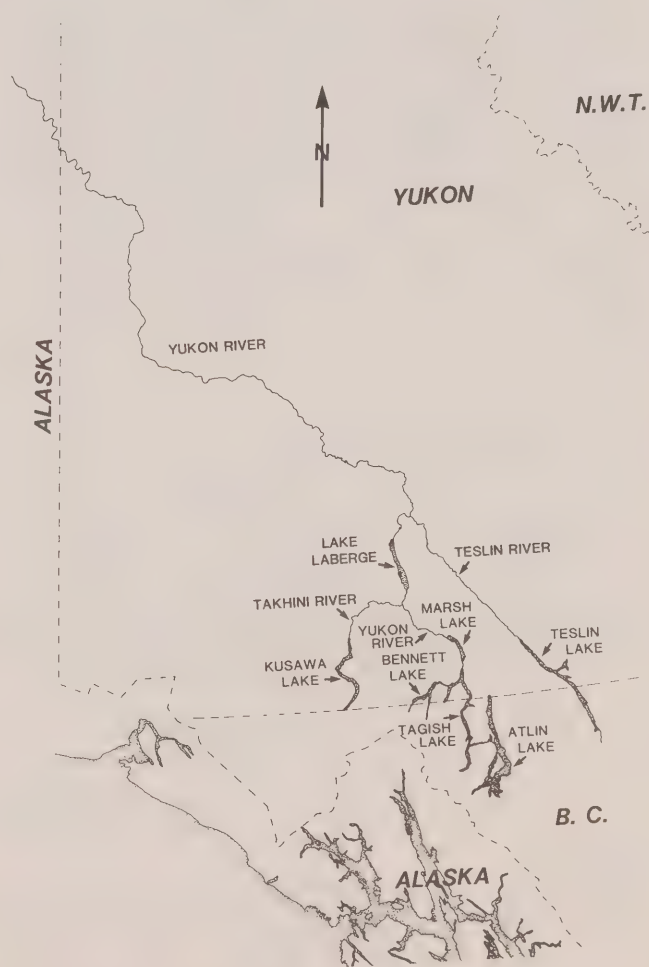


Figure 1. Yukon River basin.

for the purpose of breaking ice. The Marsh Lake dam was rebuilt in 1951/52 to provide storage; the Whitehorse Rapids dam was built in 1957/58 for hydroelectric power generation.

There are many practical and management-related problems associated with ice-covered systems that require an understanding of lake/river interaction. These include predicting changes in ice cover characteristics subsequent to alterations of natural flow conditions; estimating rates of frazil ice formation in reservoirs; mapping the dispersion of pollutants by riverine flow; maintaining open water areas as habitats for waterfowl and as staging areas for migratory birds; and ensuring optimum conditions for the overwintering of fish stock. However, as shown by omission from recent reviews on cooling processes and ice formation in lakes (e.g., Michel, 1971; Ashton, 1980, 1982; Adams, 1981; Carmack and Farmer, 1982), few studies have been carried out on the physical limnology of lakes similar to Lake Laberge, that is, large, deep lakes with continuous winter cover and a relatively large winter through-flow. There is strong evidence, however, that the winter circulation of a lake is affected by such factors as basin size (Timms, 1975; Bennett, 1978), ice cover (Scott, 1974; Adams and Lasenby, 1978), and through-flow (Wiegand and Carmack, 1982). While these factors have been identified as being important to the winter regime of lakes, very little has been done to quantify their effects or to take account of them in a unified description of the winter cycle. Hence, the Yukon Ice Seasonality Experiment (YISEX) was initiated by Environment Canada to provide basic information on the winter hydrology and limnology

of a large lake/river system (Fig. 2; also see Alford and Carmack, 1987). A pilot study was initiated in 1982/83 to obtain data on ice and snow thickness (Appendix A). This work was extended in 1983/84 to obtain hydrological, meteorological, limnological, and ice regime data for a complete winter cycle.

The present report describes the winter limnology and ice regime of Lake Laberge, using data obtained in 1983/84. Emphasis is placed on the response of the lake to external forcing, on the general problem of winter circulation under ice, and on the phenomenological requirements for numerical models of ice-covered lakes with through-flow.

LITERATURE REVIEW

The following review is intended to highlight those phenomena affecting the winter limnology and ice regime of large, deep lakes with continuous winter cover and large winter through-flow. A more general review of circulation and cooling processes in ice-covered seas and lakes is given by Carmack (1986).

Reviews of the annual cycle in temperate lakes are given in Hutchinson (1957) and Mortimer (1974). Cooling in the fall leads to a deepening of the surface mixed layer and a reduction in thermal stratification. Accounts of the initial cooling period and breakdown of stratification in temperate lakes have been given by Mortimer (1955) and Carmack and Farmer (1982), who note that the upwelling

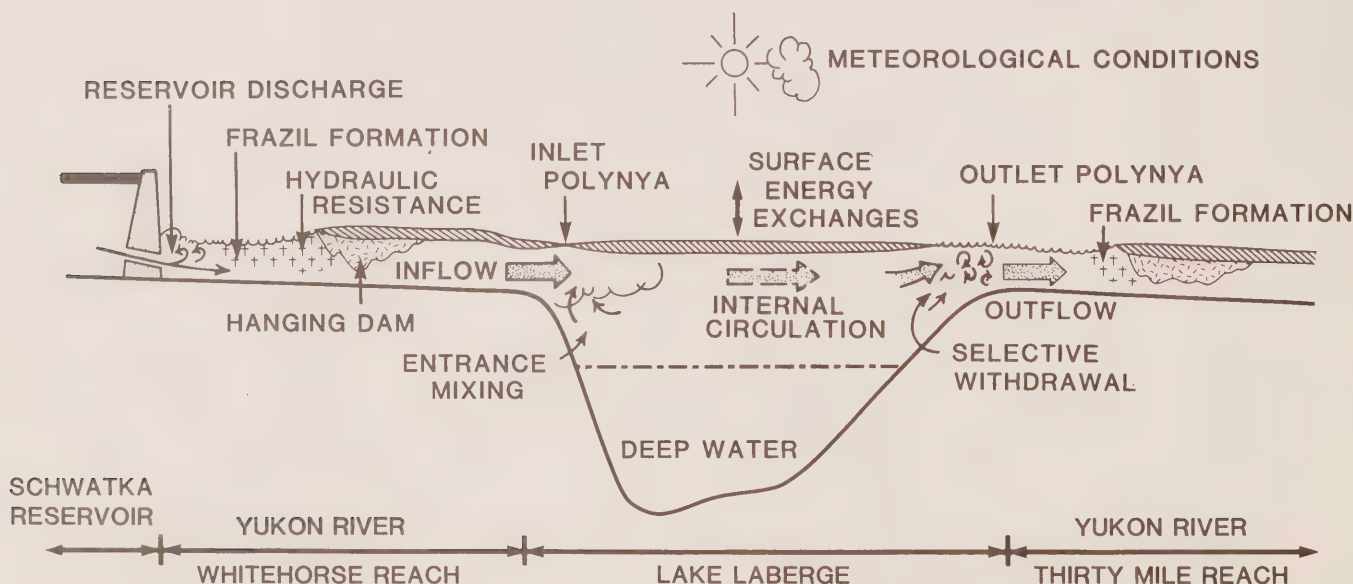


Figure 2. Schematic of YISEX.

of deeper layers at the windward end of the lake during strong winds aids vertical mixing.

As cooling proceeds, the mixed layer eventually recedes to the bottom, a condition known as lake overturn. It is often supposed that the bottom temperatures in deep lakes are at 4°C, the temperature of maximum density at 1 atm pressure. Because of wind and mechanical stirring, however, many lakes, both shallow and deep, continue to circulate until bottom temperatures are cooled well below 4°C (Yoshimura, 1936; Mortimer and Mackereth, 1958; Stewart, 1973; Scott, 1974). Wright (1931) pointed out that since the temperature of maximum density (T_M) decreases with depth, bottom temperatures in deep lakes may drop below 4°C even in the absence of wind mixing. Strom (1945) showed that many lakes exhibit a slope change in their temperature versus depth curve (i.e., temperatures increasing from 0°C at the surface to a maximum at mid-depth, and then decreasing toward the bottom). Strom believed the slope of this line represented the curve of T_M versus pressure. On this point he is probably wrong; however, we must acknowledge his observations. Johnson (1964, 1966) argued that thermodynamic processes affect the circulation of Great Bear Lake. Eklund (1963, 1965) and Bennett (1975) derived expressions for the shape of the temperature versus pressure curve using the freshwater equation of state and applying stability considerations (Eckel, 1949; Fofonoff, 1961); however, they do not explain the dynamical processes leading to a given temperature profile.

As a lake cools through 4°C, the effects of temperature on density become small and then change sign, leading to the onset of reverse stratification in which wind mixing is opposed by the positive buoyancy flux associated with cooling. Farmer and Carmack (1981) and Omstedt and Sahlberg (1983) give theoretical treatments of this situation. Farmer and Carmack (1981) also note two ways that the unique properties of fresh water influence convection at temperatures near that of maximum density. First, because of the quadratic dependence of density on temperature, the buoyancy flux depends on surface temperature as well as the rate of cooling. Second, since the temperature of maximum density decreases with depth, a reverse stratified lake may be made conditionally unstable if the base of the mixed layer is lowered to a depth where its temperature matches that of maximum density. Above this depth, the interface is stable and wind must work against buoyancy during cooling, while below it, the interface is gravitationally unstable and free convection occurs. A similar process affects the stability of deep-sea water masses (Ekman, 1934).

The timing and manner by which a lake passes through 4°C can also be influenced by spatial differences in

cooling related to bottom depth, wind exposure, or river inflow, so that lateral as well as vertical flow patterns must be taken into account (Carmack and Farmer, 1982). For example, if water at one location in a lake passes through 4°C before water at another location, a convective circulation known as the thermal bar may result. This flow occurs when warm water ($T > 4^\circ\text{C}$) mixes with cold water ($T < 4^\circ\text{C}$) to form a common, dense water mass, which then sinks along a narrow, well-defined front (Tikhomirov, 1963; Rodgers, 1965; Elliot and Elliot, 1970). Theoretical discussions of the thermal bar have been given by Huang (1972), Bennett (1971), Brooks and Lick (1972), Bowman and Okubo (1978), Scavia and Bennett (1980), and Hamblin and Ivey (1986). A general treatment of circulation in a fluid in which density extrema arise is given by Gebhart and Mollendorf (1978).

Ice formation requires a period of both cold weather and calm winds. Overviews of the thermodynamic requirements for ice formation on lakes have been published by Michel (1971), Ashton (1980, 1982), and Adams (1981). While several "freezing day" models have been described (e.g., Pivovarov, 1973), these are bulk models, which ignore lake processes. A thermodynamic model accounting for various components of surface heat exchange and ice formation was derived by Maykut and Untersteiner (1971) for oceanographic application. The influence of flow on the transfer of heat to an ice cover in rivers and lakes is discussed by Baines (1961), Gilpin *et al.* (1980), and Hamblin *et al.* (1986).

Once a stable ice cover is formed, it serves to shield the lake from further heat loss and wind stirring. Most field studies on ice-covered systems appear to have been carried out on shallow, long residence-time lakes (e.g., Woodcock, 1965; Likens and Ragotzkie, 1965; Parrott and Fleming, 1970; Palmer and Izatt, 1972; Hobie, 1973; Schindler *et al.*, 1974; Gow and Govoni, 1982). Some lakes actually warm under ice cover because of release of heat from sediments in winter (Hutchinson, 1941) or the income of solar radiation in spring (Farmer, 1975; La Perriere, 1981). Convective motion under ice can also be driven by the release of heat and dissolved substances from bottom sediments (Mortimer and Mackereth, 1958).

The optical characteristics of snow and ice cover are treated by Sherstyankin *et al.* (1970), Maguire (1975), Grenfell and Maykut (1977), Bolsenga (1981), and Roulet and Adams (1984).

Ways in which through-flow can affect the circulation and ice cover of a lake are discussed by Melin (1948), Tesaker (1973), and Bengtsson (1978, 1981). The flow of water out of a stratified lake results in upwelling near the

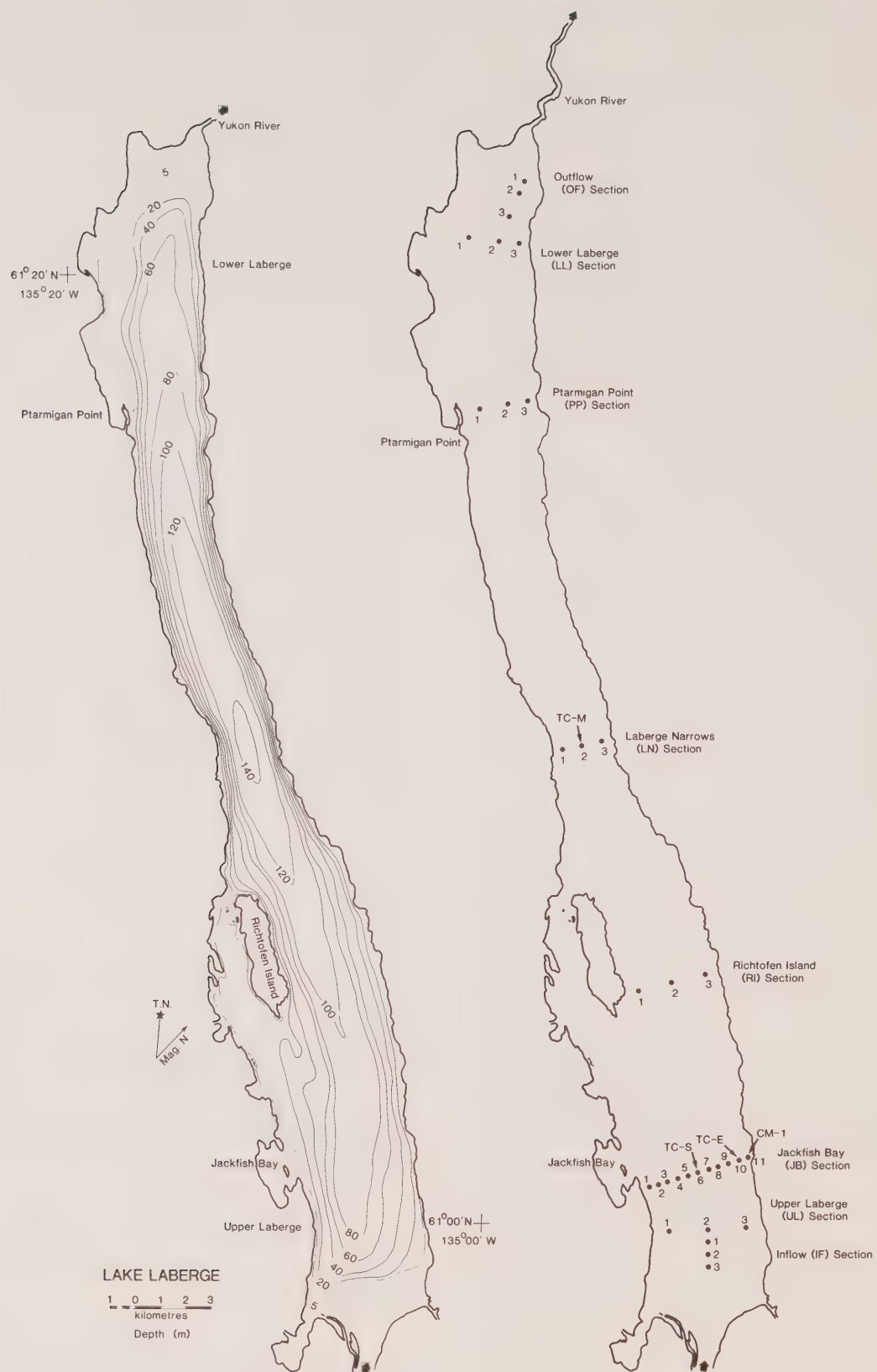


Figure 3. Lake Laberge bathymetry and station locations.

outlet, a process known as selective withdrawal (Kao, 1976; Imberger, 1980). Stewart and Martin (1982) described the distribution of inflow-derived turbidity in a small, ice-covered lake of medium residence-time.

Stigebrandt (1978) described conditions in an ice-covered lake with through-flow with respect to Lake Sperillen, Norway. He divided the lake into three regimes: the lake proper, where both internal storage and through-flow occur; the inlet region, where the mixing of inflow water occurs; and the outlet region, where the selective withdrawal of outflowing water occurs. It is in the inlet and outlet regions that strong mixing takes place and, consequently, where thin and unstable ice conditions prevail. The importance of selective withdrawal is belied by the fact that when water issues from a lake in winter, a difference of only a fraction of a degree Celsius can change the ice regime of the downstream river considerably.

With the onset of spring, the absorption of solar radiation beneath lake ice warms the underlying water. The resulting radiation-induced convection forms a deepening mixed layer that advances into the stable temperature profile below, often showing a diurnal periodicity (e.g., Farmer, 1975; Carmack, 1979). In some lakes the temperature beneath the ice may rise above 4°C (Woodcock, 1965; Williams, 1969; La Perriere, 1981).

Little attention has been given to the decay of lake ice in spring. Bilello (1980) examined several empirical approaches to predicting decay. Ashton (1983a, 1983b) discussed lake ice decay from energy budget considerations. Wake and Rumer (1979) noted that the accumulation of meltwater on the surface of ice may further complicate the heat budget of melting ice.

STUDY AREA AND METHODS

Lake Laberge is located at approximately 61° N at an elevation of 628 m. It is a long (48 km), narrow (4.2 km), deep (mean depth = 54 m) lake having a surface area of 201 km², a volume of 10.8 km³, and a basin filling time (lake volume divided by outflow) of 1.06 a.

The lake has steep sides, a flat bottom, and a U-shaped cross-sectional profile (Fig. 3). The Yukon River enters at the south end of the lake forming an inflow delta that extends about 3 km into the lake. Immediately beyond the delta break, the bottom drops with a slope of about 2.5%. The lake has a very narrow littoral zone along most of its length, with shallow water regions only at its ends, in Jackfish Bay, and behind Richtofen Island. The deepest part of the lake ($Z = 145$ m) is located in the narrow reach at mid-

length. Near the outlet the bottom rises with an average slope of 2.5%. Hypsographic curves for area and volume as functions of depth are shown in Figure 4.

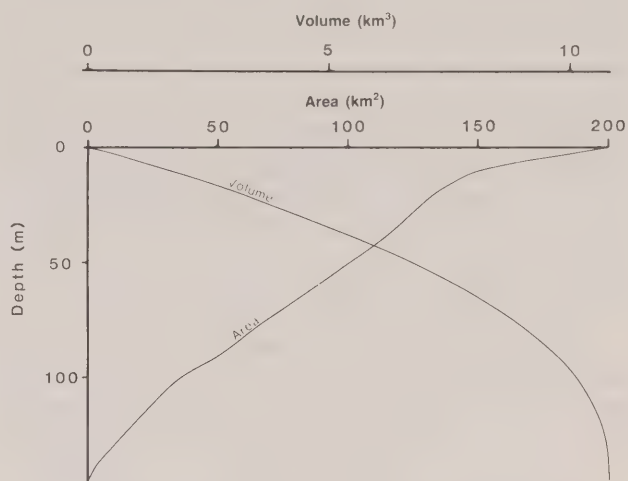


Figure 4. Area and volume as functions of depth.

The observation program was designed to obtain information on the interrelated parameters that influence ice growth and decay. Hence, a combination of techniques involving both lake surveys and remote-recording instruments was used.

Two different survey patterns were set up. To obtain detailed information on ice regime and water mass structure, a transverse section comprising 11 stations was established near Jackfish Bay and visited by snowmobile at approximately one- to two-week intervals. To obtain broader information on circulation and mixing, a lakewide survey comprising 21 stations was carried out by ski-plane at approximately one-month intervals (Marles, 1985).

At each survey station, a 0.2-m diameter hole was drilled through the ice and a vertical profile of temperature and conductivity obtained using an Applied Microsystems Model-12 conductivity-temperature-depth (CTD) probe. In turn, the CTD probe was lowered by means of a lightweight hand winch, which could be carried either in a ski-plane or on a sled. Solar radiation was measured using a Lambda Instruments light meter, which is sensitive to photosynthetically active radiation (400-700 nm). In addition, measurements were taken of ice and snow thickness, snow mass, ice thickness, and hole freeboard.

The remote-recording system included three thermistor chains, each of which recorded temperature at ten

fixed depths. Chain A was located near the southern end of the lake on the eastern side so that the temperatures recorded there would include those of riverine influence. The length of chain A was 40 m with thermistors located at 4-m intervals. Chain B was placed at the southern end of the lake, but out of the region of riverine influence. The data recorded by it should reflect the fundamental internal oscillations of the lake since the amplitude of the first mode seiche is largest at lake ends. Chain B was an 80-m chain with thermistors separated by 8 m. Chain C was located at midlake near its deepest part and was a 120-m chain with thermistors separated by 12 m. Because this site is near the node of the first mode seiche, changes in thermal structure here will reflect more on the seasonal meteorological forcing of the lake than on the internal seiching.

A meteorological station made by Aanderaa Instruments was set up near the inlet. This instrument recorded solar radiation, wind velocity, air temperature, water temperature, and relative humidity. Data were recorded on magnetic tape at either 30- or 60-minute intervals. A propane-heated enclosure was built to house the data recorder, thus allowing operation at temperatures down to -50°C . The water temperature sensor was lost, however, when ice movement at freeze-up sheared the connecting cable.

Daily values of cloud cover were obtained from the Atmospheric Environment Service observatory in Whitehorse.

ENVIRONMENTAL PARAMETERS

Hydrology

The total area of the Yukon River basin upstream from Lake Laberge is $25\,385\text{ km}^2$. The mean annual streamflow is $10.2\text{ km}^3\text{ a}^{-1}$; of this about 90% is drawn from the surface layers of upstream lakes. The average water yield for the basin upstream from the lake is 0.4 m a^{-1} .

The hydrograph of the outflow from Lake Laberge is shown in Figure 5. The mean annual discharge is $325\text{ m}^3\text{ s}^{-1}$. Minimum flows are observed in winter between January and March. Streamflow increases rapidly from May onwards, reaching a maximum in August and September. This late summer peak in streamflow is characteristic of a basin that receives much of its runoff from glacial melt. Streamflows observed in 1983/84 were slightly lower than the long-term trend.

While there is certainly an annual cycle to the hydrograph, it is not an overly large one, with the summer discharge being only five or six times that of the winter dis-

charge. This is because Lake Laberge draws much of its water from natural storage in upstream lakes, a source that persists year-round. Year-to-year variations, however, are substantial because of fluctuations in rainfall and snow and glacier melt.

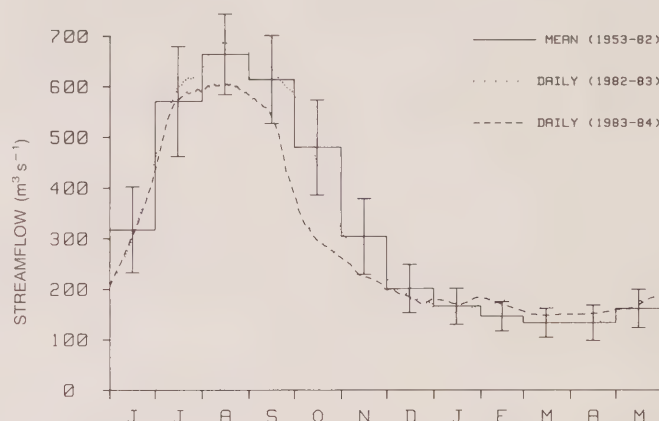


Figure 5. Streamflow of the Yukon River out of Lake Laberge. (Vertical bars denote standard deviation.)

The lake level varies by 2 to 3 m throughout the year (Fig. 6), with maximum levels in August and minimum levels in March. During the period of ice cover (December through May), however, there is very little fluctuation in water level. In considering the water balance of Lake Laberge, it is important to take into account lake level fluctuations. During periods of high flow, there is a storage flux, defined as the difference between inflow and outflow, of almost $60\text{ m}^3\text{ s}^{-1}$. In winter, however, water levels are almost constant and the storage flux can be disregarded.

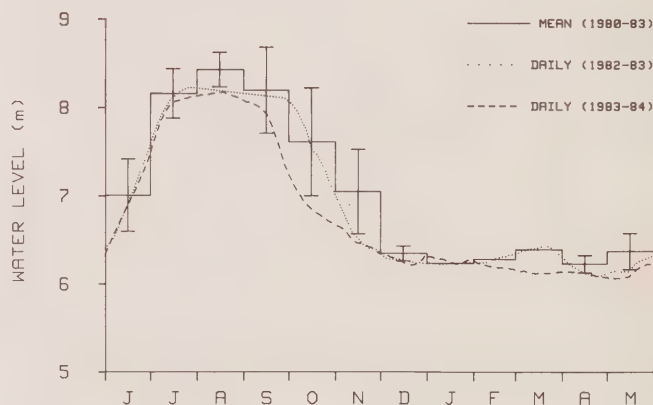


Figure 6. Water level of Lake Laberge. (Vertical bars denote standard deviation.)

Ice and Snow Cover

Typically, Lake Laberge is frozen from late December to early June. Plots of mean ice thickness as a function of time for 1983/84 (Fig. 7) show rapid change during freeze-up and breakup, and gradual change in midwinter. The mid-winter equilibrium thickness is 0.8 to 1.0 m. Visual inspection of ice thickness profiles across the Jackfish Bay section (not shown) reveals no clear pattern across the lake. This latter observation is in contrast to that of Tesaker (1973), who observed that in Lake Sperillen the thinnest ice occurred along the right-hand shoreline (relative to river inflow).

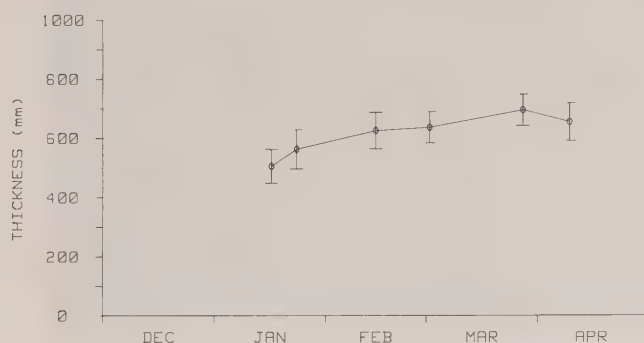


Figure 7. Mean ice thickness at the Jackfish Bay section.

Anomalous ice conditions exist at the inlet and outlet of the lake (Figs. 8 and 9) because of enhanced vertical mixing in these areas. A portion of the outlet area is always ice free; we will refer to this area as the outlet polynya. The inlet area, however, may either be open or consist of thin and irregular ice. This topic is discussed further in a later section.

The seasonal ice regime is strongly affected by the physical properties of the snow cover. This is because snow increases the weight on ice, alters the albedo, and adds conductive insulation to the underlying ice and water.

Figure 10 shows the mean snow depth at the Jackfish Bay section in 1983/84. Figure 11 shows the relation between snow depth (obtained from snow cores on the lake) and snow mass (obtained by melting snow cores and measuring the equivalent water depth). Typically, the snow is about 10% water.

Figure 12 shows the relation between snow mass and the deficit water level. This latter quantity is obtained by subtracting the measured freeboard (distance from water level to ice surface) from the theoretical freeboard (calculated for free-floating ice), and is thus the amount the ice



Figure 8. Ice conditions at the inlet of Lake Laberge.



Figure 9. Ice conditions at the outlet of Lake Laberge.

surface is depressed below its hydrostatic water level. If at any given station the snow mass accounts for the deficit, then the correlation point would lie on a 45-degree line, indicating one-to-one correspondence. In the present case, the points tend to lie slightly below the 45-degree line, suggesting that the ice is weakly suspended.

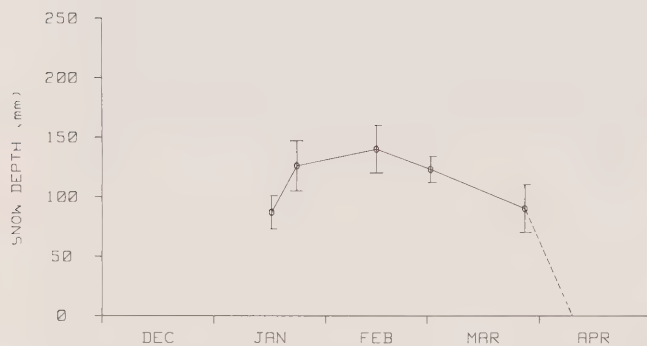


Figure 10. Mean snow depth at the Jackfish Bay section.

The relation between incident and reflected solar radiation (Fig. 13) shows that during most of the winter the albedo is about 0.75. In late spring, however, the albedo falls to about 0.30.

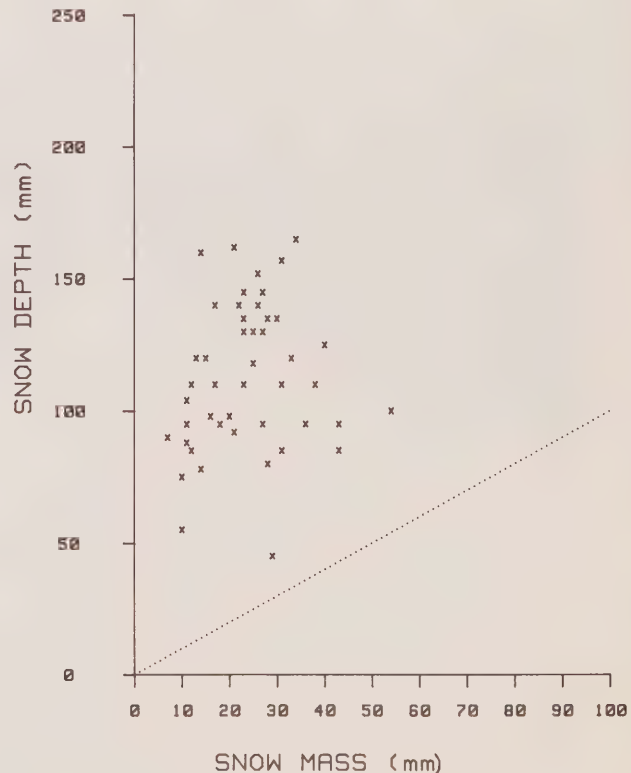


Figure 11. Snow depth in relation to equivalent snow mass at the Jackfish Bay section.

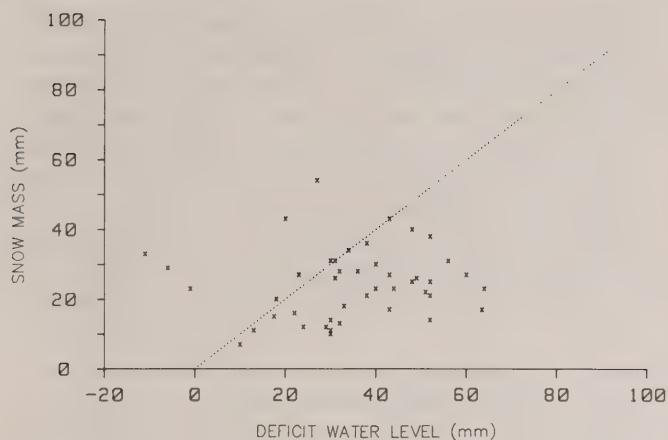


Figure 12. Snow mass in relation to the deficit water level at the Jackfish Bay section.

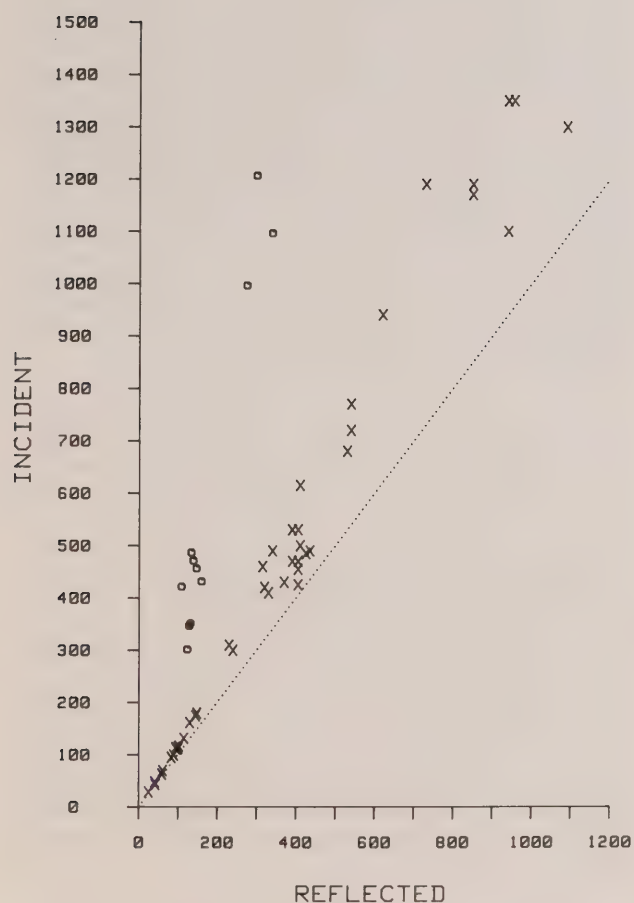


Figure 13. Incident solar radiation in relation to reflected solar radiation at the Jackfish Bay section. (The symbol *o* is used to distinguish measurements obtained during the April transect under conditions of no snow cover.)

The relation between solar radiation at the ice/water interface and at 1 m depth (Fig. 14) shows that 25% of the radiation entering the upper water column is absorbed in the top 1 m. This penetration can be expressed in terms of an extinction coefficient k , defined by $I(z) = I_W \exp[-kz]$, where $I(z)$ is radiation at a specified depth, and I_W is radiation at the ice/water interface; a mean value for k is about 0.3.

Meteorology

Appendix B, Figures B-1 to B-5, shows plots of wind velocity, solar radiation (net shortwave), air temperature, relative humidity, and cloud cover as functions of time. Wind strength is related to synoptic (1- to 2-week) weather patterns, and is generally constrained along the axis of the lake. Air temperature and solar radiation are clearly dominated by seasonal trends, while relative humidity and cloud cover exhibit strong day-to-day variability.

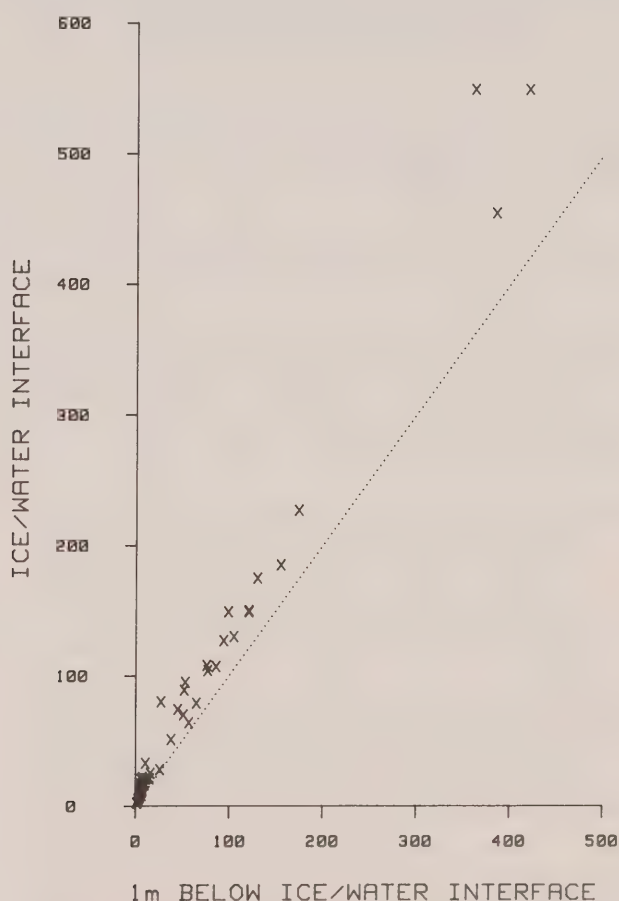


Figure 14. Solar radiation at the ice/water interface in relation to solar radiation 1 m below the ice/water interface at the Jackfish Bay section.

WINTER TEMPERATURE STRUCTURE

Forcing Parameters

Circulation and mixing within the lake are forced by the wind W , by river through-flow R , and by surface heat exchange Q . Following Fisher *et al.* (1979), the influence of the wind is given by the turbulent friction velocity $w_* = (\tau/\rho_w)^{1/2}$, defined in terms of the wind stress $\tau = C_d \rho_a W^2$ ($\text{kg m}^{-1} \text{s}^{-2}$), where C_d is the drag coefficient (1.3×10^{-3}), and ρ_w and ρ_a are the densities of water ($999.975 \text{ kg m}^{-3}$) and air (1.2 kg m^{-3}), respectively. By analogy, the influence of river through-flow is given by the turbulent advection velocity $r_* = (C_d u_r^2)^{1/2}$, where u_r is the mean velocity of river through-flow (see Wiegand and Carmack, 1982). Finally, the influence of surface cooling is given by the turbulent convection velocity $q_* = (Bh_1)^{1/3}$, defined in terms of the buoyancy flux $B = g\alpha Q(c_p \rho_w)^{-1}$ ($\text{m}^2 \text{s}^{-3}$), where Q is the surface heat flux, α is the coefficient of thermal expansion ($68 \times 10^{-4} \text{ }^\circ\text{C}^{-1}$ at $8 \text{ }^\circ\text{C}$), and c_p is the specific heat ($4194 \text{ J kg}^{-1} \text{ }^\circ\text{C}^{-1}$). In the present case the surface heat flux is computed from the observed change in heat content as a function of time (see below).

Note that w_* is only meaningful prior to freeze-up, while b_* is only meaningful during periods when heat exchange promotes convection.

A comparison of the turbulent velocity scales (Appendix C, Figs. C-1 to C-3) shows the following features.

- (1) During late summer and early fall, w_* is generally the dominant fluctuating component, with typical values of 0.002 to 0.005 m s^{-1} and maximum values approaching 0.010 m s^{-1} . When the continuous ice cover forms, w_* vanishes.
- (2) During fall (prior to overturn and surface temperatures above 4°C), b_* has a value comparable to w_* , with typical values in the range of 0.004 to 0.006 m s^{-1} . Cooling at temperatures below 4°C adds buoyancy to the lake, and hence b_* vanishes.
- (3) The r_* term is small, of order 0.002 or less. During the period of full ice cover, however, when both w_* and b_* vanish, r_* becomes the dominant source of turbulence.

Thermal History

The thermal history of the lake was recorded by three thermistor chains. Chain A was a 40-m chain located near

the southern end of the lake on the eastern side so that the temperatures recorded there would include those of riverine influence. Chain B was an 80-m chain placed at the southern end of the lake, but out of the region of riverine influence. The data recorded by it should reflect the fundamental (first mode) internal seiche. Chain C was a 120-m chain located at midlake near its deepest part. Because this site is near the node of the first mode seiche, changes in thermal structure here will reflect more on the seasonal meteorological forcing of the lake than on the internal seiching.

To describe the seasonal temperature structure of Lake Laberge, thermistor chain data were plotted both as isotherm depth as a function of time (Appendix D, Fig. D-1) and as daily mean profiles (Appendix D, Fig. D-2). A summary of the seasonal temperature structure, based on bimonthly mean profiles, is shown in Appendix D, Figure D-3. It should be noted here that the depths plotted are accurate to within 2 m. Visual inspection of these plots in relation to the external forcing parameters leads to the following description.

The first three weeks of September reveal the lake to contain large amplitude (30- to 40-m, peak-to-peak) oscillations, which are associated with the first-mode internal seiche. They are most notable in data from A and B at the end of the lake and are missing in data from C at the middle station, the latter being located near the node for this mode. Instead, C contains waves of shorter period (about 2 days) with an antiphase relationship to the motion at B, and likely associated with a binodal seiche. The amplitude of the seiche increases towards the end of the month, possibly because of partial resonance with the wind.

During the last week of September, storm winds (Appendix B, Fig. B-1) around the 20th radically modify the thermal structure, which is then further disturbed during a wind reversal on the 26th. Hence, at the beginning of October, the lake has a much deeper, cooler surface mixed layer. Large amplitude, wind-driven seiching is still prominent with a strong north wind driving isotherms to the bottom at the southern end of the lake on October 4. Thereafter the lake gradually cools its large surface layer with occasional assistance from the wind. Isotherms progressively bend upward and disappear from the lake. A sharp increase in the depth of the isotherms immediately before their surfacing, together with a slight warming of the bottom layers, indicates some degree of penetrative convection.

Overturn, where the lake is essentially isothermal at a temperature near 4°C , takes place in early November and occurs at the shallower stations first.

While the main body of the lake is in full circulation, further cooling results in inverse stratification in shallower portions first, as evidenced by the isotherms from stations A and B. Winds are light for most of the last three weeks of November and into the first week of December so that as the lake continues to cool, the stratification continues. From December 5 to 10, the isotherms are severely depressed by strong winds out of the north, which together with extreme low temperatures further cool the lake. On December 10 the winds drop, and ice is seen to form on the lake's surface.

With the formation of an ice cover, the lake is shielded from the wind. The subsequent rebound of the isotherms is gradual and with virtually no overshoot, resembling very much a damped wave. By December 21 no evidence of the seiche remains.

At the beginning of January 1984, the lake has a fairly level thermal structure, although with some evidence of small amplitude internal motions, especially at the mid-lake station. These small motions may be related to atmospheric pressure disturbances, to instabilities in the through-flow circulation, or to disturbances associated with the inflow and outflow. The movement of the isotherms is not necessarily coherent and there is some evidence of spreading isotherms, indicating higher vertical mode internal waves. Bottom waters tend to warm up as the month progresses, with some evidence of a fairly large amplitude (10 m) wave in the deepest portions of the lake. This trend in bottom temperature continues through February. Upper isotherms from the southern end of the lake are mainly flat, although at midlake some wave motion occurs. Motion below the 3°C isotherm is antiphase with that occurring above, so a higher vertical mode seiche is indicated here also. Through March, however, the lake becomes quiet and there is virtually no motion of the isotherms.

In April we begin to see gradual but notable warming at all stations as cooler isotherms rise and disappear from surface waters. This is coincident with the breakup and warming of the upstream river (Alford and Carmack, 1987) so that warming of the lake is affected by the inflow. As well there is some indication of episodes of diurnal (penetrative) convection at C. Indications of internal seiching appear at station B as the isotherms rise and then fall during the month in a slow undulation. This wave motion continues into May with increasing amplitude. In addition, there is a strong indication of penetrative convection during the second week in May, especially at station C.

On 15 May there is a dramatic increase in internal wave activity at all stations. Since the lake is still ice-covered at this time, this behaviour is difficult to explain.

We note, however, that this is the date inflow begins to rise. Also, inflow temperatures now are above 4°C, so that the cabbeling instability is operative.

Heat continues to penetrate the lake as it nears spring overturn in the early weeks of June. Breakup occurs during the first week of June, after which time the lake stratifies. Note that the onset of stratification is aided by the down-lake spreading of river water, so that stratification develops first at A, then at B, and finally at C (Carmack *et al.*, 1979).

Heat Budget

The approach taken here is one of directly calculating the total heat flux as the rate of change of heat content in the lake. To do this, data from the midlake thermistor chain are used as an indicator of the lakewide average temperature profile. Obviously, data from only one location are likely to be aliased by internal waves; however, this error should be minimal at midlake, where the amplitude of the first mode internal seiche is presumed to be small.

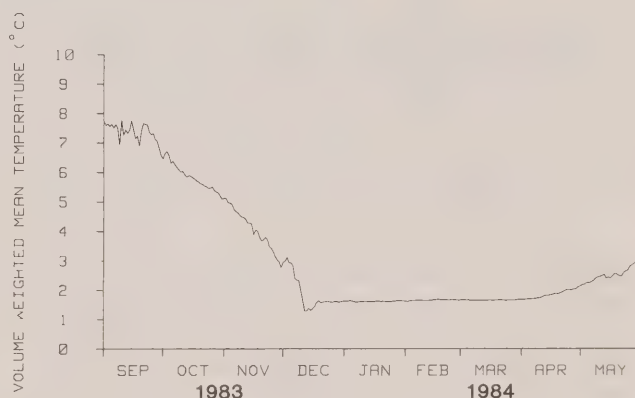


Figure 15. Volume-weighted mean temperature as a function of time.

The volume-weighted mean temperature of Lake Laberge as a function of time is shown in Figure 15. The corresponding heat content at any given time is $H = \rho_w c_p V \langle T \rangle$, where V is lake volume ($10.8 \times 10^9 \text{ m}^3$) and $\langle T \rangle$ is the volume-weighted mean temperature at any given time. The high frequency fluctuations in Figure 15 are likely associated with internal wave activity, and are thus disregarded. The following annual trend is noted. Prior to freeze-up in mid-December the mean cooling rate is $0.067^\circ\text{C d}^{-1}$. Throughout midwinter the mean temperature remains nearly constant because of the insulating effect of the ice cover. Warming commences in late April because of the penetration of solar radiation through the ice cover and the influx of warm river water.

The corresponding heat flux (computed from the rate of change of volume-weighted mean temperature and latent heat) as a function of time is shown in Figure 16. Again ignoring high frequency fluctuations caused by internal waves, the fall heat flux is observed to be about 175 to 200 W m^{-2} . In midwinter the heat flux computed from the change in heat content is small. However, taking the latent heat flux into account during the initial period of ice formation, an additional flux of order 100 W m^{-2} is obtained.



Figure 16. Heat flux (computed from the rate of change of volume-weighted mean temperature and latent heat) as a function of time.

THROUGH-FLOW AND WATER MASS FORMATION

The movement of river water through a lake during winter affects heat exchange, ice thickness, and the dispersion of material (Melin, 1948; Tesaker, 1973; Stigebrandt, 1978; Svensson and Larsson, 1980; Hamblin *et al.*, 1986). Still, very little is known about riverine circulation in ice-covered lakes because of the very small velocities involved. For example, suppose the inflow of $150 \text{ m}^3 \text{ s}^{-1}$ moves through the upper 15 m of the lake in a 2-km wide current. Dividing the flow by the cross-sectional area yields a velocity of order 0.005 m s^{-1} , or about 400 m d^{-1} .

Some idea of the expected riverine circulation can be gained from physical considerations. Since the inflow has a temperature near 0°C , its density is less than that of lake water, and thus must spread as a buoyant plume within the upper layers of the lake. If the flow is further assumed to be influenced by Coriolis forces, it may be treated as a boundary gravity current (Griffiths, 1986). Theoretical and laboratory studies of such currents show they propagate only with a boundary on their right-hand side (in the northern hemisphere). In Lake Laberge this means that the riverine flow should be most intense along the eastern margin of the lake ("right margification"). However, the

current is also acted on by frictional resistance, both at the ice/water interface and at lower levels. This effects an Ekman-type transport of water away from the eastern margin of the lake, which tends to broaden the current downlake (Stigebrandt, 1978; Svensson and Larsson, 1980).

Using these physical considerations as guidelines, and taking into account the small speeds involved, property distributions are next examined as a way of inferring circulation patterns.

Temperature and Conductivity Sections

Transverse sections of temperature (T) and conductivity relative to 25°C (C_{25}) across the lake at Jackfish Bay at various times in winter are shown in Appendix E, Figure E-1. This section is approximately 7 km from the river mouth and 4 km from the delta break.

Throughout winter the lake exhibits reverse stratification with temperature increasing monotonically with depth. The largest temperature gradient (winter thermocline) lies at 30 to 45 m depth between the 1.2°C and 2.0°C isotherms. Here the vertical gradient of temperature is about $0.05^\circ\text{C m}^{-1}$, and the vertical gradient of density, $d\rho/dz$, is about 0.002 kg m^{-4} . Here, density is computed using the equation of state given by Chen and Millero (1977). The buoyancy frequency, which determines the upper frequency limit for internal wave motions, is defined as $N = [(g/\rho)(d\rho/dz)]^{1/2}$. Within the winter thermocline, this parameter has values of about $0.5 \times 10^{-2} \text{ s}^{-1}$. Isotherms within and above the thermocline show a weak tendency to be concave upwards, while deeper isotherms tend to slope upward toward the east shore.

During winter the temperature of inflow water remains colder and less dense than lake water, so it tends to spread in the upper layers of the lake. In addition, the conductivity of inflow water increases in winter. These two characteristics affect the C_{25} distribution. For example, almost all variability in C_{25} occurs above the winter thermocline. A curious feature is the persistent occurrence of isolated conductivity inversions at midlake immediately above the thermocline.

Sections of T and C_{25} along the axis of the lake are shown in Appendix E, Figure E-2. Note here that the isopleths of temperature and conductivity are essentially level except for distortions near the inlet and outlet. For example, isotherms near the inlet are typically concave upwards and centred at the JB section, while isotherms show a strong tendency to diverge beginning near the LL section. Conceivably, these distortions reflect geostrophic readjustment in the through-flow.

The February 14 section shows a near-bottom layer of high C_{25} water at the south end of the lake. The source of this layer is presently unknown. It is clearly not of river origin because of its high temperature. It may be related, however, to the release of dissolved solids from sediments in a manner similar to that described by Mortimer and Mackereth (1958).

Temperature and Conductivity Correlation Diagrams

Correlation diagrams are widely used by oceanographers to identify and trace water masses (see Mamayev, 1975, for review). If the plotted data on such a diagram fall on a straight line, then the mixing is supposed to be between the two end-member water masses, to be conservative in that no external sources or sinks exist, and to be steady in that the properties of the end-member constituents remain constant over a time period longer than the flushing time of the system. However, if a curved or broken line results, then either several water masses exist, the mixing involves non-conservative properties, or the system is unsteady (Loder and Reichard, 1981). Keeping these general guidelines in mind, we will examine the observed temperature/conductivity (T/C_{25}) correlation curves from Lake Laberge.

Figure 17 shows the family of T/C_{25} curves from three midlake stations for each of the three lakewide surveys. While some individual variation exists, one feature is clear, namely, the break in the individual curves that occurs at temperatures between 0.8°C and 1.6°C . This break takes place at lower temperatures (shallower depths) with distance downlake. The T/C_{25} break is easily understood from the point of view of an unsteady mixing model, taking into account the seasonality of the conductivity of river water. At overturn the lake was presumably well mixed; hence the entire lake would exist as one point (4°C , $92\ \mu\text{S m}^{-1}$) on the correlation plot. Then, as the surface of the lake cooled and froze, the T/C_{25} curve would appear as a vertical line extending down $92\ \mu\text{S m}^{-1}$ from 0°C to about 4°C . With no external inputs (i.e., in steady state), the lake would retain this T/C_{25} structure throughout the winter. However, the river adds cold, high conductivity water to the system on a time scale commensurate with the residence time of the upper layers of the lake. Because of this variation in end-member concentration with time, the T/C_{25} curve develops a bend that broadens through the winter.

A conclusion that follows from this analysis is that the break in the T/C_{25} curve represents the maximum depth of water influenced by winter inflow, i.e., the depth of the riverine layer. We will refer to this break as the water

mass boundary, and to the water above this break as the moving layer.

Horizontal Property Distributions

The use of water property maps to infer horizontal circulation relies on the assumption that the main pathways of flow from source regions result in patterns or tongues in the property distributions. The approach is to first define a meaningful mapping surface for the water mass in question, and then to examine the distribution of some variable or tracer on that surface in relation to a known source.

In the present case, we examine two surfaces that relate to the riverine layer: the 0.5°C isothermal surface and the base of the water mass boundary defined above. The 0.5°C isothermal surface was chosen for mapping because it lies within the riverine layer, it closely approximates an isopycnal surface, and temperature may be treated as a nearly conservative property in winter. For this surface we plot its depth and the distribution of C_{25} (Appendix F, Figs. F-1 to F-3).

The T/C_{25} break was chosen as a second mapping surface because it appears to be the best indication of the base of the riverine layer. For this surface we plot its depth and the corresponding distribution of temperature (Appendix F, Figs. F-4 to F-6). From these maps the following general patterns are noted.

- (1) There is a tendency for the depths of both the 0.5°C surface and the water mass boundary to be deeper at the south end of the lake than at the north, and to be deeper along the east shore than along the west. This is consistent with the notion of a river-induced flow that initiates from the south end of the lake and flows along the east shore. The latter behaviour is likely a consequence of the Coriolis force.
- (2) Conductivity on the 0.5°C surface exhibits a weak tendency to decrease from south to north and from east to west. Again, this is consistent with the idea of a riverine flow that moves preferentially along its right-hand shoreline in the direction of flow.
- (3) Temperature on the water mass boundary tends toward higher temperatures along the south and east boundaries of the lake. Further, there is a gradual warming of this surface through winter. This behaviour suggests that the effects of entrainment of ambient lake water into the riverine layer is more advanced near the inflow, and that the entraining front slowly deepens through winter.

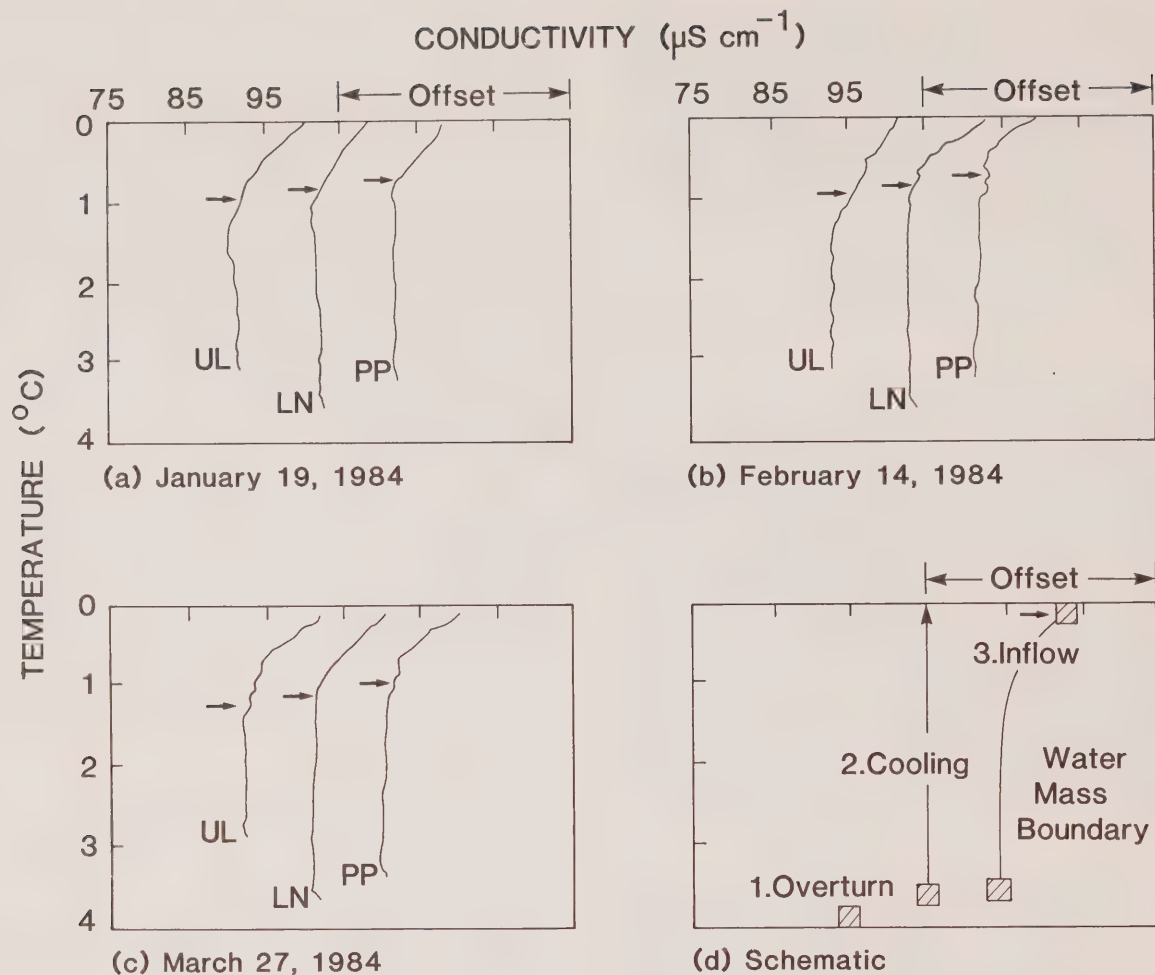


Figure 17. T/C_{25} correlation curves at three midlake stations for each of the three lakewide surveys and schematic diagram showing T/C_{25} curve evolution arising from through-flow. Curves in each plot are offset by $10 \mu\text{S cm}^{-1}$; arrows denote the approximate position of the water mass boundary.

Inlet Dynamics

As noted earlier, an area of open water or thin ice invariably occurs in the vicinity of the inlet immediately beyond the delta break (Fig. 8). While the delta break itself is very broad, about 3 km, the zone of thin ice is narrow, about 200 m. This is because during winter the water level in the lake drops over 2 m, and freezing drops the effective water level an additional 1 m. This means that most of the delta face is covered with landfast ice. Hence, the winter inflow must enter the lake by means of one or more pro-deltaic conduits. As a result, the flow is strongly channelized (Fig. 18), and the velocity of water entering the lake may actually be higher in winter than in summer, even though the total streamflow is much less.

The consequences of this situation are illustrated by observations obtained in the area and shown in Figure 19.

River water meets the lake moving through the conduit with velocities near 1 m s^{-1} (Fig. 19c). Upon entering the lake, this water spreads at the surface as a buoyant, turbulent jet. Here the entrainment of ambient lake water due to turbulence and enhanced vertical heat transfer caused by horizontal velocity near the ice/water boundary combine to produce a narrow zone of thin ice extending into the lake.

Additional evidence of strong mixing near the inlet jet is given by temperature profiles obtained from the area shown in Figure 19a. These profiles (Fig. 20) display temperature inversions that decrease in intensity with distance from the point of inflow. Indication that the intensity of turbulent mixing decreases with distance from the point of inflow is also shown in profiles of the vertical density gradient (Fig. 21). Stations near the inlet show negative values, evidence of overturning by mechanical stirring.



Figure 18. Pro-deltaic channels in the inlet.

The inflow domain may be treated as a turbulent jet in a stratified fluid (Jirka *et al.*, 1981; Chu and Baddour, 1984). In this case the jet has characteristic features of length $L_0 = 800$ m, width $b_0 = 200$ m, and initial velocity

$v_0 = 0.8 \text{ m s}^{-1}$. Because the jet extends farther than one Rossby radius into the lake and lies farther than one Rossby radius from a boundary, anticyclonic eddies are likely formed and shed at the jet's tip.

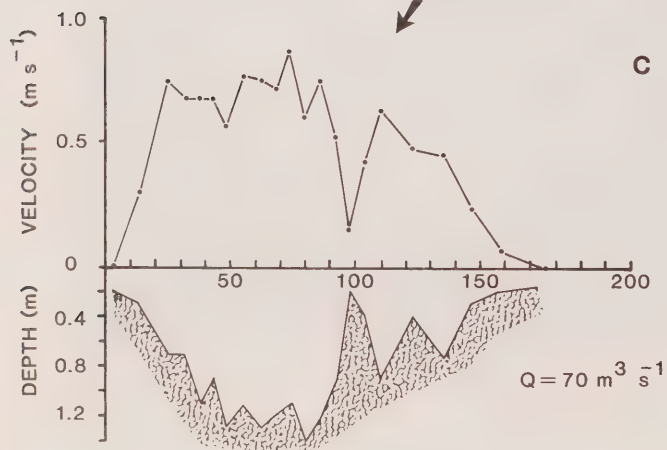
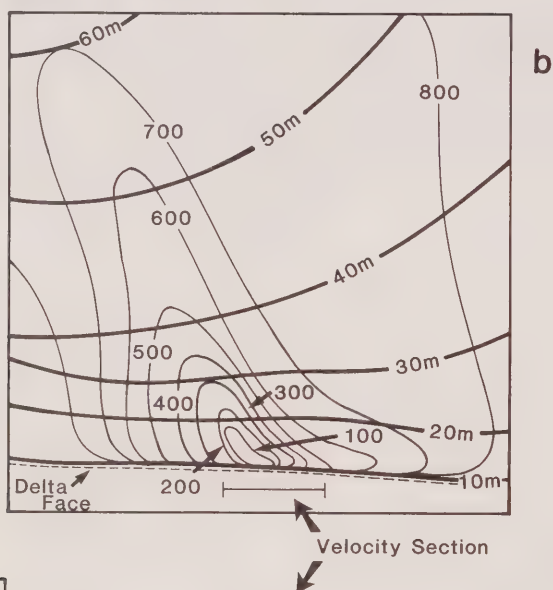
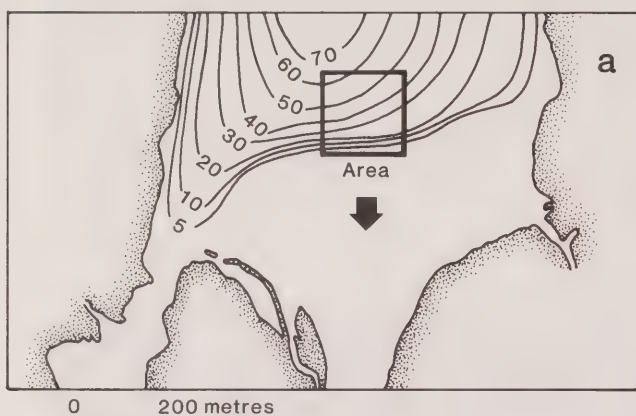


Figure 19. Plots showing (a) study area for the inlet survey, (b) ice thickness and water depth, and (c) the horizontal profile of velocity at the inlet.

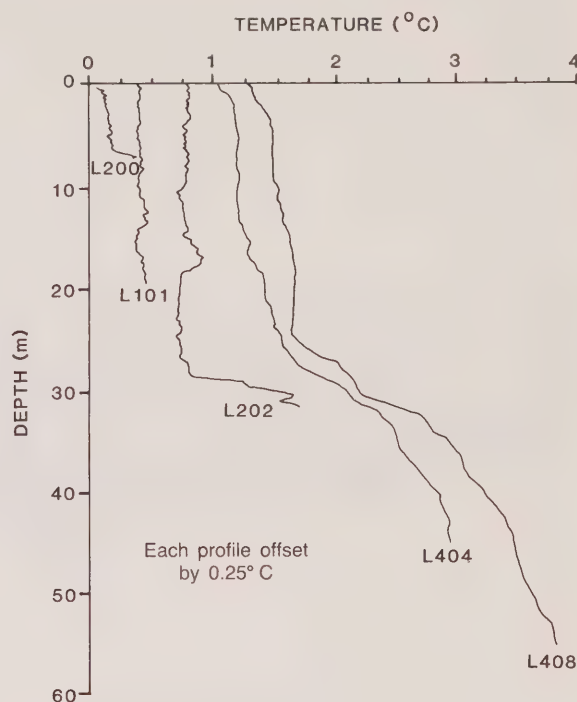


Figure 20. Temperature near the inlet.

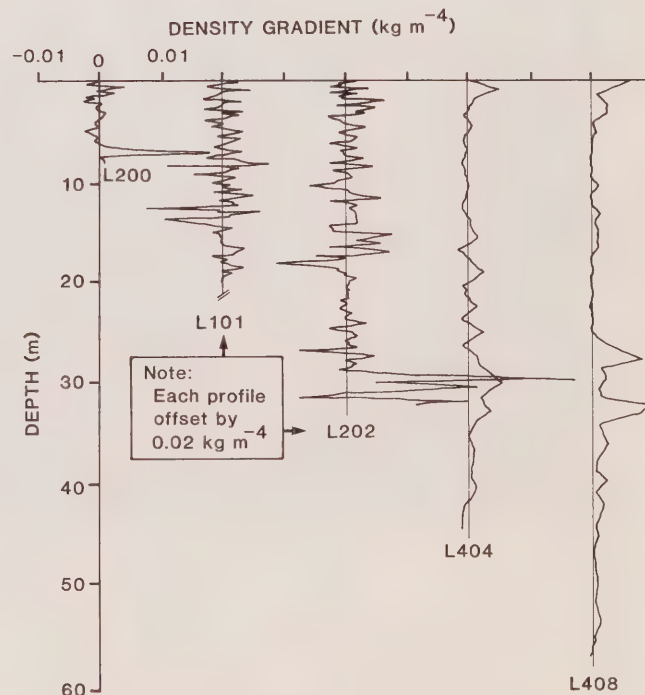


Figure 21. Density gradient near the inlet.

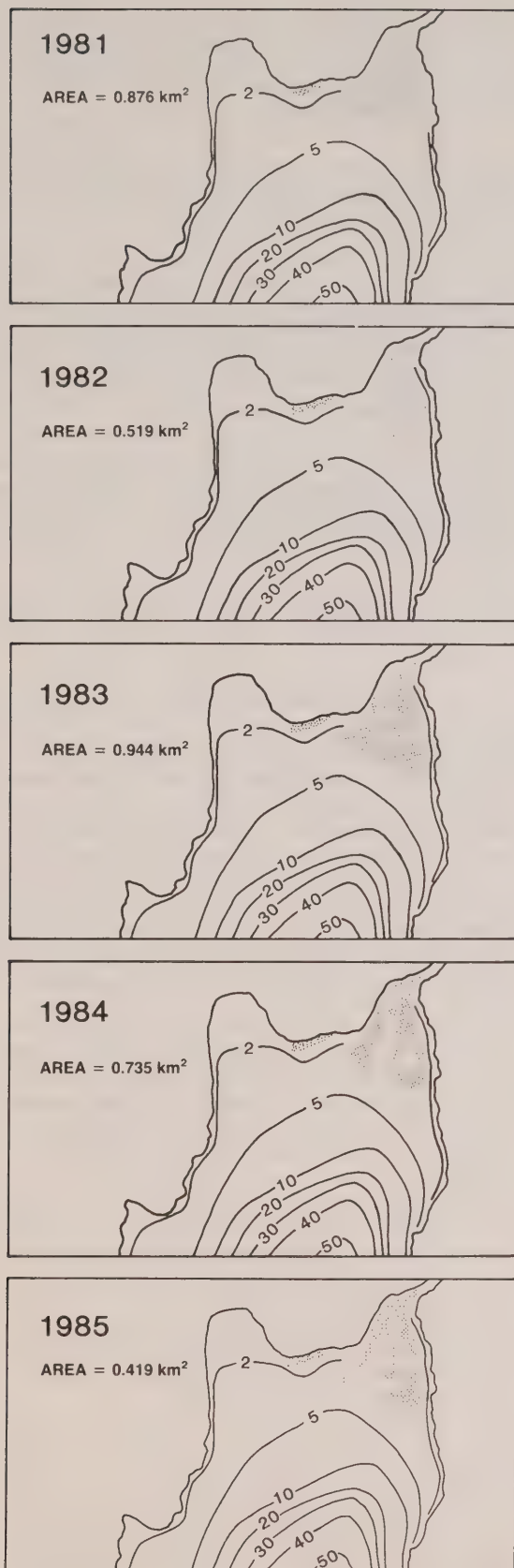


Figure 22. Open water surface area at the outlet.

Outlet Dynamics

The outlet areas of ice-covered lakes are very important from an ecological point of view. The open water area or polynya is a critical habitat for overwintering waterfowl. The region of thin ice surrounding the polynya is subject to breakup earlier than the main lake, and thus serves as an early staging area for migratory birds. Because of upwelling, clarity of water, and a stable substrate, lake outlets are also fairly productive areas.

Maps of open water surface area in midwinter for the period 1981 to 1985 (Fig. 22) show an average ice-free area of 0.70 km² (0.22 km² std. dev.). The outer boundary of the polynya is fairly constant from year to year, suggesting it is largely controlled by the interaction of flow with bathymetry (also, see Hamblin *et al.*, 1986).

A section of temperature approaching the outlet obtained in March 1983 is shown in Figure 23. Isotherms remain relatively flat up to within about 2 km of the outlet. At this point isotherms above 20 m depth are disturbed. In particular, temperatures and temperature gradients in the upper 6 to 8 m of the lake increase, while deeper temperatures and temperature gradient decrease. The near-surface effects relate to flow convergence and upwelling. The deeper effects are probably caused by mixing at the bottom and the establishment of a return (uplake) flow below the outflowing water.

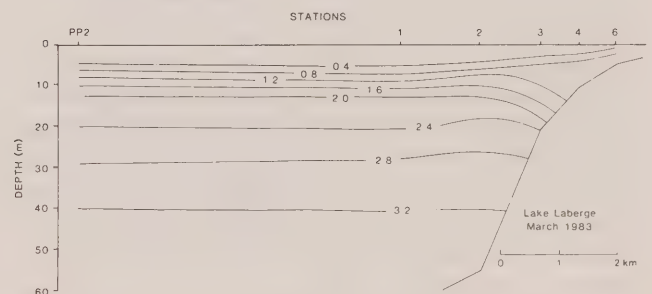


Figure 23. Temperature section near the outlet.

Stigebrandt (1978) gives an equation for computing the withdrawal depth for surface outflows, $h_0 = 1_0 (Q^2/N^2 B_0^2 D_0)^{1/3}$, where 1_0 is a constant (0.74), Q is streamflow, N is the buoyancy frequency, and B_0 and D_0 are the width and depth of the lake at its outflow. Taking values appropriate to the midwinter outflow of Lake Laberge (i.e., $Q = 150 \text{ m}^3 \text{ s}^{-1}$, $B_0 = 200 \text{ m}$, $D_0 = 3 \text{ m}$, and $N = 5 \times 10^{-2} \text{ s}^{-1}$), we find $h_0 = 15 \text{ m}$. While it does not appear that water from this depth is actually leaving the lake (Fig. 23), it is close to the depth that isotherms are disturbed by the outflow circulation.

DISCUSSION

Because of its winter through-flow, Lake Laberge also has many of the physical characteristics of a deep, ice-covered reservoir. Thus it can be used as a prototype for developing numerical models of both lake and reservoir systems, providing that the dominant physical processes are identified.

What has been done with regard to the numerical modeling of stratification (e.g., thermal structure) in ice-covered lakes with through-flow? Several "freezing day" models have been described (e.g., Pivovarov, 1972). These are bulk models, however, which ignore lake processes. Sundaram and Rehm (1973), Rahman (1978), Killworth and Carmack (1979), and Omstedt and Sahlberg (1983) developed temperature structure models for the period of reverse stratification, but did not include ice formation. Svensson and Larsson (1980) discussed the turbulent Ekman layer in an ice-covered lake, but again omitted ice growth and decay. Wake and Rumer (1979) and Brossia *et al.* (1981) developed models directed at surface ice formation, but neglected the thermodynamic coupling between the ice cover and the underlying water. Patterson and Hamblin (1986) coupled the thermodynamic ice/snow model of Maykut and Untersteiner (1971) with a lake mixing model originally developed by Imberger *et al.* (1978) using the boundary layer parameterization of Hamblin *et al.* (1986). Because the model is one-dimensional (1-D), however, the effects of inflow, through-flow, and outflow circulation require further parameterization.

At this point it should be apparent that there are tremendous difficulties in constructing realistic 1-D models of the winter regime of northern lakes and reservoirs. Based on the present study of Lake Laberge, it would appear that certain processes and events are of general significance with regard to the winter limnology and ice regime of a large northern lake with winter ice cover and through-flow.

- (1) As lakes cool toward 4°C, they become strongly two- and three-dimensional in character in that large spatial differences in circulation and mixing may occur. These features must be properly parameterized to allow their effects to be incorporated in a 1-D model.
- (2) To model the wintertime stratification in deep lakes properly, it is also necessary to incorporate two thermodynamic properties of fresh water: first, that the temperature of maximum density decreases with depth; and second, that the compressibility of cold water is greater than that of warm water.

- (3) The initial freeze-over period is extremely complex, and the criteria for ice-cover formation under a balance of varying wind, snowfall, and cooling conditions is still unknown.
- (4) The behaviour of through-flow, including mixing at inlet and outlet regions, must be understood before proper parameterization is possible.
- (5) The general problem of water movement under ice, e.g., the gravitational circulation associated with the generation of horizontal density gradients, is important since it results in a significant redistribution of water masses.
- (6) A proper treatment of ice decay requires consideration of the optical properties of ice and snow, of convection in the underlying water, and of the physical evolution of the ice itself.

REFERENCES

- Adams, W.P. 1981. Snow and ice on lakes. In *Handbook of Snow: Principles, Processes, Management Use*, ed. D.M. Gray and D.H. Hale, pp. 437-74. New York: Pergamon Press.
- Adams, W.P., and D.C. Lasenby. 1978. The role of ice and snow in lake heat budgets. *Limnol. Oceanogr.*, 23: 1025-28.
- Alford, M.E., and E.C. Carmack. 1987. Observations on ice cover and streamflow in the Yukon River near Whitehorse during 1983/84. NHRI Pap. No. 32, Sci. Ser. No. 152, National Hydrology Research Institute, National Hydrology Research Centre, Inland Waters/Lands Directorate, Environment Canada, Saskatoon, Sask.
- Ashton, G.D. 1980. Freshwater ice growth, motion and decay. In *Dynamics of Snow and Ice Masses*, ed. S. Colbeck, pp. 261-304. New York: Academic Press.
- Ashton, G.D. 1982. Theory of thermal control and prevention of ice in rivers and lakes. *Adv. Hydrosol.*, 13: 131-85.
- Ashton, G.D. 1983a. Lake ice decay. *Cold Reg. Sci. Technol.*, 8: 83-86.
- Ashton, G.D. 1983b. First-generation model of ice deterioration. In *Frontiers in Hydraulic Engineering*, ed. H.T. Shen, pp. 273-77. Am. Soc. Civ. Eng., New York.
- Baines, W.D. 1961. On the transfer of heat from a river to an ice sheet. *Trans. Eng. Inst. Can.*, 5: 27-32.
- Bengtsson, L. 1978. Winter stratification in a lake dominated by through-flow. In *Modelling of Dynamic Phenomena in Lakes*, ed. L. Bengtsson, Div. Water Resour. Eng. Ser. A, No. 10, pp. 24-45. University of Lulea, Sweden.
- Bengtsson, L. 1981. Experiences on the winter thermal regimes of rivers and lakes with emphasis on Scandinavian conditions. In *Proc. Int. Symp. Ice*, Quebec, pp. 11-54.
- Bennett, E.B. 1975. Evidence of minimum potential energy as a constraint on large-scale mixing in oceans and lakes. Canada Centre for Inland Waters, Environment Canada, Burlington, Ont. Unpub. ms.

- Bennett, E.B. 1978. Characteristics of the thermal regime of Lake Superior. *J. Great Lakes Res.*, 4: 310-19.
- Bennett, J.R. 1971. Thermally driven lake currents during the spring and fall transition periods. In *Proc. 14th Conf. Great Lakes Res.*, Int. Assoc. Great Lakes Res., Ann Arbor, Mich., pp. 535-44.
- Bilello, M.A. 1980. Maximum thickness and subsequent thickness of lake, river, and fast sea ice in Canada and Alaska. Report 80-6, U.S. Army Corps Eng. Cold Reg. Res. Eng. Lab., Hanover, N.H.
- Bolsenga, S.J. 1981. Radiation transmittance through lake ice in the 400-700 nm range. *J. Glaciol.*, 27: 57-66.
- Bowman, M.J., and A. Okubo. 1978. Cabbelling at thermohaline fronts. *J. Geophys. Res.*, 83: 6173-78.
- Brooks, I., and W. Lick. 1972. Lake currents associated with the thermal bar. *J. Geophys. Res.*, 77: 6000-13.
- Brossia, M. de, J.M. Baldasano, and B. Coupal. 1981. Modelling the formation and melting of ice cover. In *Simulating the Environmental Impact of a Large Hydroelectric Project*, ed. N. Therien, pp. 39-43. Society for Computer Simulation, La Jolla, Calif.
- Carmack, E.C. 1979. Combined influence of inflow and lake temperatures on spring circulation in a riverine lake. *J. Phys. Oceanogr.*, 9: 422-34.
- Carmack, E.C. 1986. Circulation in ice-covered waters. In *Air-Sea-Ice Interaction*, ed. N.J. Untersteiner, NATO Advanced Study Institute. Seattle: University of Washington Press. In press.
- Carmack, E.C., and D.M. Farmer. 1982. Cooling processes in deep, temperate lakes: a review with examples from two lakes in British Columbia. *J. Mar. Res.*, 40 (Supplement): 85-111.
- Carmack, E.C., C.B.J. Gray, C.H. Pharo, and R.J. Daley. 1979. Importance of lake-river interaction on seasonal patterns in the general circulation of Kamloops Lake. *Limnol. Oceanogr.*, 24: 634-44.
- Chen, C.T., and F.J. Millero. 1977. The use and misuse of pure water PVT properties for lake waters. *Nature*, 266: 707-8.
- Chu, V.C., and R.E. Baddour. 1984. Turbulent gravity-stratified shear flows. *J. Fluid Mech.*, 138: 353-78.
- Eckel, O. 1949. Über die Mischungsarbeit von Stabil Geschichteten Wassermassen. *Arch. Meteorol. Geophys. Bioklimatol.*, 1: 264-69.
- Eklund, H. 1963. Fresh water: temperature of maximum density calculated from compressibility. *Science*, 142: 1457-58.
- Eklund, H. 1965. Stability of lakes near the temperature of maximum density. *Science*, 149: 632-33.
- Ekman, V.W. 1934. George Wüst: Das Bodenwasser und die Gliederung der Atlantischen Tiefsee. *J. Cons.*, 9: 192-94.
- Elliot, G.H., and J.A. Elliot. 1970. Laboratory studies on the thermal bar. In *Proc. 13th Conf. Great Lakes Res.*, Int. Assoc. Great Lakes Res., Ann Arbor, Mich., pp. 413-18.
- Farmer, D.M. 1975. Penetrative convection in the absence of mean shear. *Q. J. R. Meteorol. Soc.*, 101: 869-91.
- Farmer, D.M., and E.C. Carmack. 1981. Wind mixing and restratification in a lake near the temperature of maximum density. *J. Phys. Oceanogr.*, 11: 1516-33.
- Fisher, H.B., E.J. List, R.C.Y. Koh, J. Imberger, and N.H. Brooks. 1979. *Mixing in Inland and Coastal Waters*. New York: Academic Press.
- Fofonoff, N.P. 1961. Energy transformations in the sea. *Fish Res. Board Can.*, Ms. Rep. Ser. 109.
- Gebhart, B., and J.C. Mollendorf. 1978. Buoyancy induced flows in water under conditions in which density extrema may arise. *J. Fluid Mech.*, 89: 673-707.
- Gilpin, R.R., T. Hirata, and K.C. Cheng. 1980. Wave formation and heat transfer at an ice-water interface in the presence of a turbulent flow. *J. Fluid Mech.*, 89: 619-40.
- Gow, A.J., and J. Govoni. 1982. Observations and analysis of Post Pond ice growth. Report 82-00. U.S. Army Corps Eng. Cold Reg. Res. Eng. Lab., Hanover, N.H.
- Grenfell, T.C., and G.A. Maykut. 1977. The optical properties of ice and snow in the arctic basin. *J. Glaciol.*, 18: 445-63.
- Griffiths, R.W. 1986. Gravity currents in rotating systems. *Annu. Rev. Fluid Mech.*, 18: 59-89.
- Hamblin, P.F., E.C. Carmack, and Y.R. Marmoush. 1986. On the rate of transfer of heat between a lake and an ice sheet. Submitted for publication in *J. Geophys. Res.*
- Hamblin, P.F., and G. Ivey. Convection near the temperature of maximum density due to horizontal temperature differences. In preparation.
- Hobie, J.E. 1973. Arctic limnology: a review. In *Alaskan Arctic Tundra*, ed. M.E. Britton, pp. 127-68. Arct. Inst. North Am., Tech. Pap. 25.
- Huang, J.C. 1972. The thermal bar. *Geophys. Fluid Dyn.*, 3: 1-25.
- Hutchinson, G.E. 1941. Limnological studies in Connecticut. IV. The mechanism of intermediary metabolism in stratified lakes. *Ecol. Monogr.*, 11: 21-60.
- Hutchinson, G.E. 1957. *A Treatise on Limnology*, Vol. 1. New York: Wiley.
- Imberger, J. 1980. Selective withdrawal: a review. In *Proc. 2nd Int. Symp. Stratified Flows*, ed. T. Carstens and T. McClimans, pp. 381-400. Trondheim: Tapir Press.
- Imberger, J., J. Patterson, B. Hebbert, and I. Loh. 1978. Dynamics of reservoir of medium size. *J. Hydraulic. Div., Am Soc. Civ. Eng.*, 104: 725-43.
- Jirka, G.H., E.E. Adams, and K.D. Stolzenbach. 1981. Buoyant surface jets. *J. Hydraul. Div. Am. Soc. Civ. Eng.*, 107: 1467-87.
- Johnson, L. 1964. Temperature regime of deep lakes. *Science*, 144: 1336-37.
- Johnson, L. 1966. Temperature of maximum density of fresh water and its effects on the circulation in Great Bear Lake. *J. Fish. Res. Board Can.*, 23: 725-43.
- Kao, T.W. 1976. Selective withdrawal criteria of stratified fluids. *J. Hydraul. Div., Am. Soc. Civ. Eng.*, 102: 717-29.
- Killworth, P.D., and E.C. Carmack. 1979. A filling-box model of river-dominated lakes. *Limnol. Oceanogr.*, 24: 201-17.
- La Perriere, J.D. 1981. Vernal overturn and stratification of a deep lake in the high subarctic under ice. *Verh. Int. Ver. Theor. Angew. Limnol.*, 21: 288-92.
- Likens, G.E., and R.A. Ragotzkie. 1965. Vertical water motions in a small ice-covered lake. *J. Geophys. Res.*, 70: 2333-44.
- Loder, T.C., and R.P. Reichard. 1981. The dynamics of conservative mixing in estuaries. *Estuaries*, 4: 64-69.
- Maguire, R.J. 1975. Light transmission through snow and ice. *Tech. Bull. No. 91*, Canada Centre for Inland Waters, Inland Waters Directorate, Environment Canada, Burlington, Ont.
- Mamayev, O.I. 1975. *Temperature-Salinity Analysis of World Ocean Waters*. Amsterdam: Elsevier.
- Marles, E.M. 1985. Limnological survey techniques from small aircraft. *Tech. Bull. No. 139*, National Water Research Institute, Pacific and Yukon Region, Inland Waters Directorate, Environment Canada, Vancouver, B.C.
- Maykut, G.A., and N. Untersteiner. 1971. Some results from a time-dependent thermodynamic model of sea ice. *J. Geophys. Res.*, 76: 1550-75.
- Melin, R. 1948. Currents caused by water flowing through lakes. In *P. V. Assemb. Gen. Oslo*, Union Geod. Geophys. Int., pp. 373-77.

- Michel, B. 1971. Winter regime of rivers and lakes. Monograph III-B1a, U.S. Army Corps Eng. Cold Reg. Res. Eng. Lab., Hanover, N.H.
- Mortimer, C.H. 1955. The dynamics of autumn overturn in a lake. Publ. Assoc. Hydrol. Assemb. Gen. Roma, 3: 13-24.
- Mortimer, C.H. 1974. Lake hydrodynamics. Mitt. Int. Ver. Theor. Angew. Limnol., 20: 124-27.
- Mortimer, C.H., and F.J.H. Mackereth. 1958. Convection and its consequences in ice-covered lakes. Verh. Int. Ver. Theor. Angew. Limnol., 13: 923-32.
- Omstedt, A., and J. Sahlberg. 1983. Measured and numerically-simulated autumn cooling in the Bay of Bothnia. Tellus, 35: 231-40.
- Palmer, M.D., and J.B. Izatt. 1972. Lake movements with partial ice cover. Limnol. Oceanogr., 17: 403-9.
- Parrott, W.H., and W.M. Fleming. 1970. The temperature structure of a mid-latitude, dimictic lake during freezing, ice cover and thawing. Report DA Task 1T061101A91A, U.S. Army Corps Eng. Cold Reg. Res. Eng. Lab., Hanover, N.H.
- Patterson, J., and P.F. Hamblin. 1986. Thermal simulation of a lake with winter ice cover. Submitted for publication in Limnol. Oceanogr.
- Pivovarov, A.A. 1972. Thermal conditions in freezing lakes and rivers. Izdatel'stvo Moskovskogo Universiteta. Trans. Israel Program for Scientific Translations Ltd. Jerusalem: Keter Publishing House.
- Rahman, M. 1978. On thermal stratification in reservoirs during the winter season. Water Resour. Res., 14: 377-80.
- Rodgers, G.K. 1965. The thermal bar of the Laurentian Great Lakes. In Proc. 8th Conf. Great Lakes Res., Int. Assoc. Great Lakes Res., Ann Arbor, Mich., pp. 358-63.
- Roulet, N.T., and W.P. Adams. 1984. Illustration of the spatial variability of light entering a lake using an empirical model. Hydrobiologia, 109: 67-74.
- Scavia, D., and J.R. Bennett. 1980. Spring transition period in Lake Ontario—a numerical study of the causes of large biological and chemical gradients. Can. J. Fish. Aquatic Sci., 37: 823-33.
- Schindler, D.W., H.E. Welch, J. Kalff, G.J. Brunskill, and N. Kritsch. 1974. Physical and chemical limnology of Char Lake, Cornwallis Island. J. Fish. Res. Board Can., 31: 585-607.
- Scott, J.T. 1974. A comparison of the heat balance of lakes in winter. Tech. Rep. 13, Department of Meteorology, University of Wisconsin, Madison, Wisc.
- Sherstyankin, P.P., V.M. Kaplin, and V.N. Maksimov. 1970. Vertical distribution of transparency in Lake Baikal during the under-ice period, and its relation to biological characteristics. Hydrobiol. J., 8: 50-52.
- Stewart, K.M. 1973. Winter conditions in Lake Erie with reference to ice and thermal structure and comparisons to Lakes Winnebago (Wisconsin) and Mille Lacs (Minnesota). In Proc. 16th Conf. Great Lakes Res., Int. Assoc. Great Lakes Res., Ann Arbor, Mich., pp. 845-57.
- Stewart, K.M., and P.J.H. Martin. 1982. Turbidity and its causes in a narrow glacial lake with winter ice cover. Limnol. Oceanogr., 27: 510-17.
- Stigebrandt, A. 1978. Dynamics of an ice-covered lake with through-flow. Nord. Hydrol., 9: 219-44.
- Strom, K.M. 1945. The temperature of maximum density of fresh waters. Geofys. Publ., 16: 1-14.
- Sundaram, T.R., and R.G. Rehm. 1973. The seasonal thermal structure of deep temperate lakes. Tellus, 25: 157-67.
- Svensson, U., and R. Larsson. 1980. A one-dimensional numerical study of some basic features of the flow in ice-covered lakes. J. Hydraul. Res., 18: 251-67.
- Tesaker, E. 1973. Horizontal cross-flow temperature gradients in a lake due to Coriolis' force. Hydrol. Lakes Symp., Int. Assoc. Hydrol. Sci., Helsinki, pp. 72-80.
- Tikhomirov, A.I. 1963. The thermal bar in Lake Lodoga. Izv. Akad. Nauk. SSSR Ser. Geogr., 95: 134-42. Trans. Am. Geophys. Union, Soviet Hydrol. Sel. Pap., No. 2.
- Timms, B.V. 1975. Morphometric control of variation in annual heat budget. Limnol. Oceanogr., 11: 110-12.
- Wake, A., and R.R. Rumer. 1979. Effects of surface melt-water accumulation on the dissipation of lake ice. Water Resour. Res., 15: 430-34.
- Wiegand, R.C., and E.C. Carmack. 1982. Seasonal aspects of the surface advective heat fluxes of Kootenay Lake, British Columbia. Water Resour. Res., 18: 1493-1502.
- Williams, G.P. 1969. Water temperature during the melting of lake ice. Water Resour. Res., 5: 1134-38.
- Woodcock, A.H. 1965. Melt patterns in ice over shallow waters. Limnol. Oceanogr., 10 (Supplement): R290-R297.
- Wright, S. 1931. Bottom temperatures in deep lakes. Science, 74: 413.
- Yoshimura, S. 1936. A contribution to the knowledge of deep water temperatures of Japanese lakes. Part. II. Winter temperatures. Jpn. J. Astron. Geophys., 14: 57-83.

Appendix A
Data from the 1982/83 Pilot Study

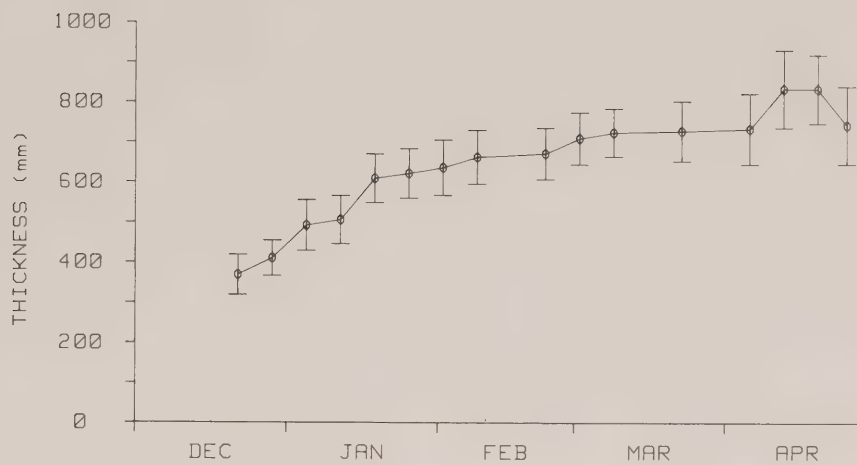


Figure A-1. Mean ice thickness at the Jackfish Bay section.

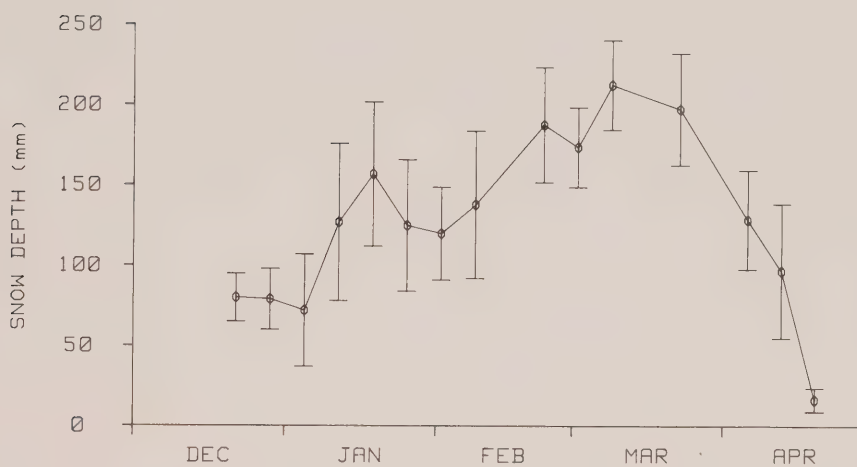


Figure A-2. Mean snow depth at the Jackfish Bay section.

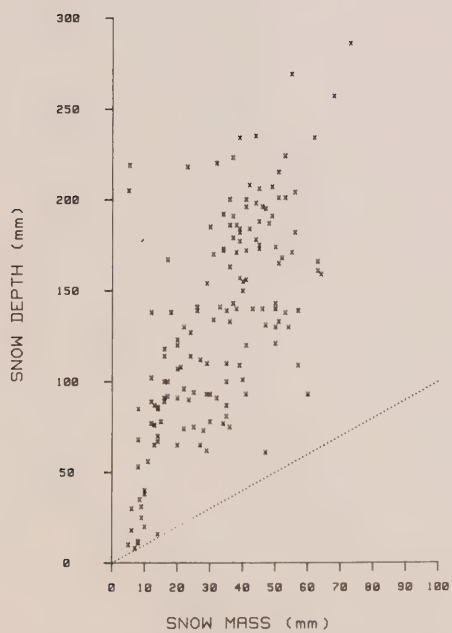


Figure A-3. Snow depth in relation to equivalent snow mass at the Jackfish Bay section.

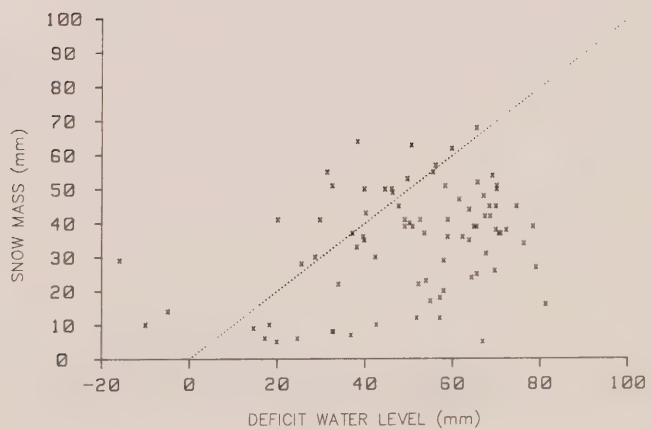


Figure A-4. Snow mass in relation to the deficit water level at the Jackfish Bay section.

Appendix B

Meteorological Data

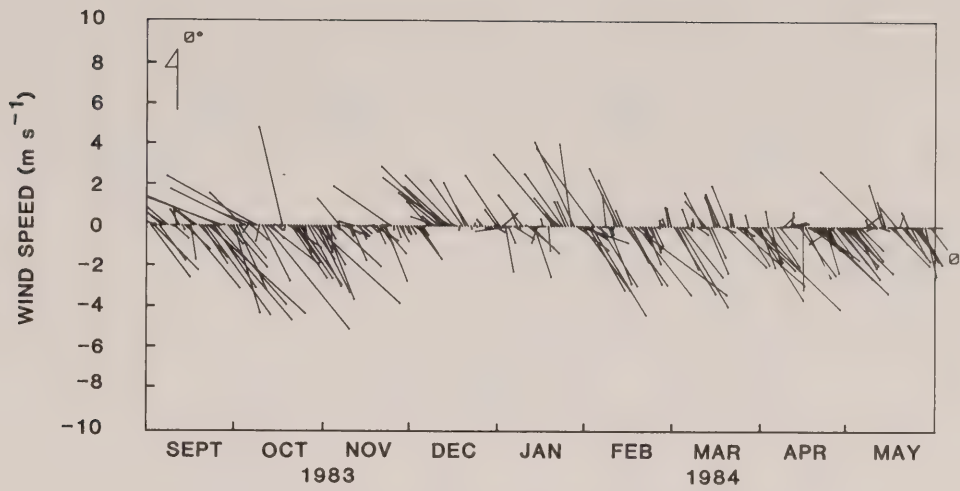


Figure B-1. Wind velocity at the Lake Laberge meteorological station.

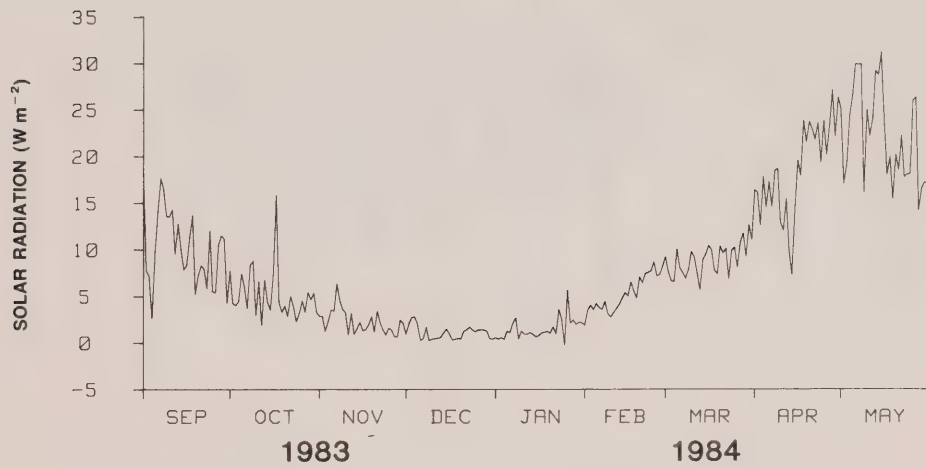


Figure B-2. Solar radiation at the Lake Laberge meteorological station.

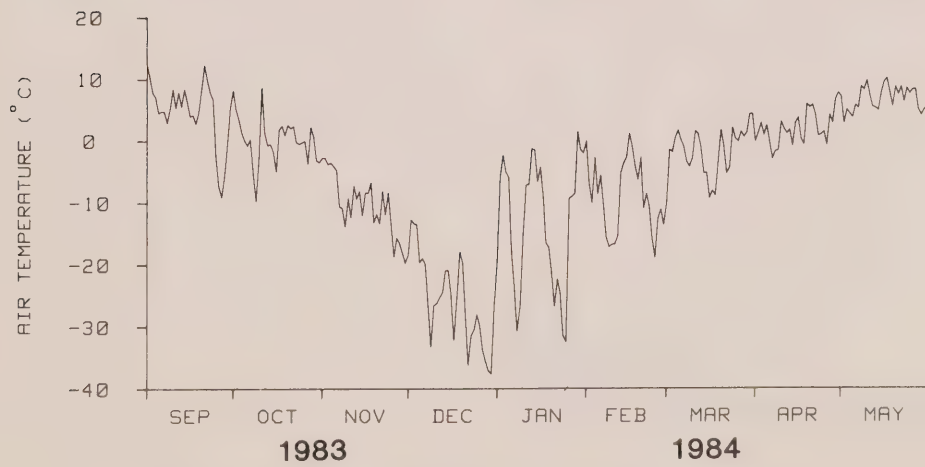


Figure B-3. Air temperature at the Lake Laberge meteorological station.

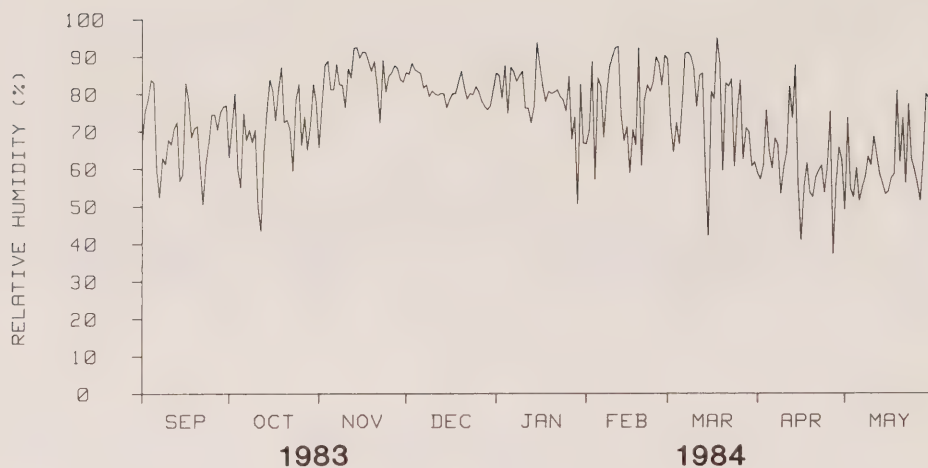


Figure B-4. Relative humidity at the Lake Laberge meteorological station.

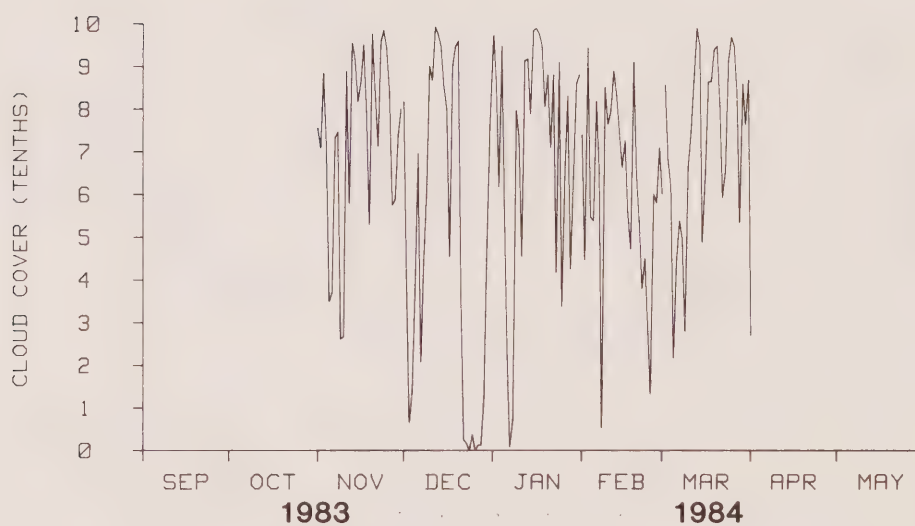


Figure B-5. Cloud cover at Whitehorse.

Appendix C

Turbulent Velocity Scales

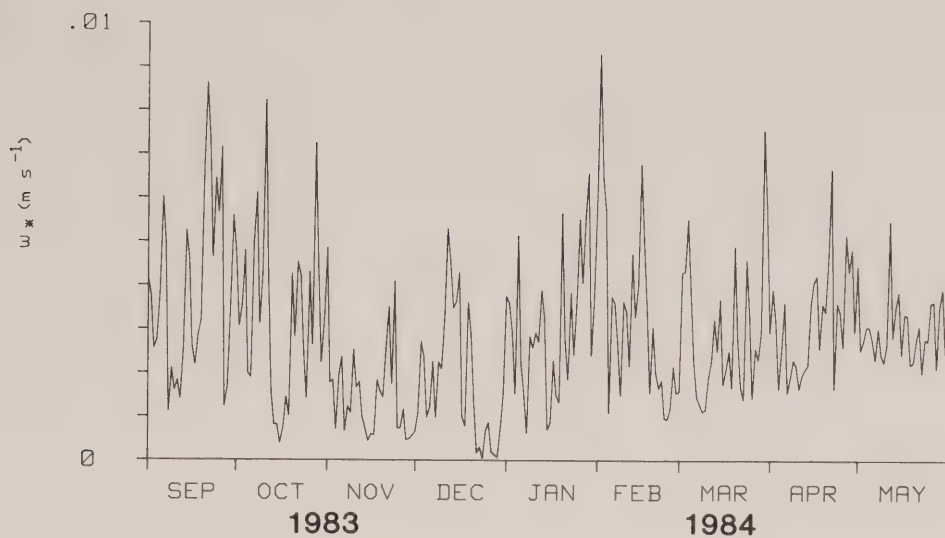


Figure C-1. The forcing parameter w_* (until freeze-up) as a function of time.

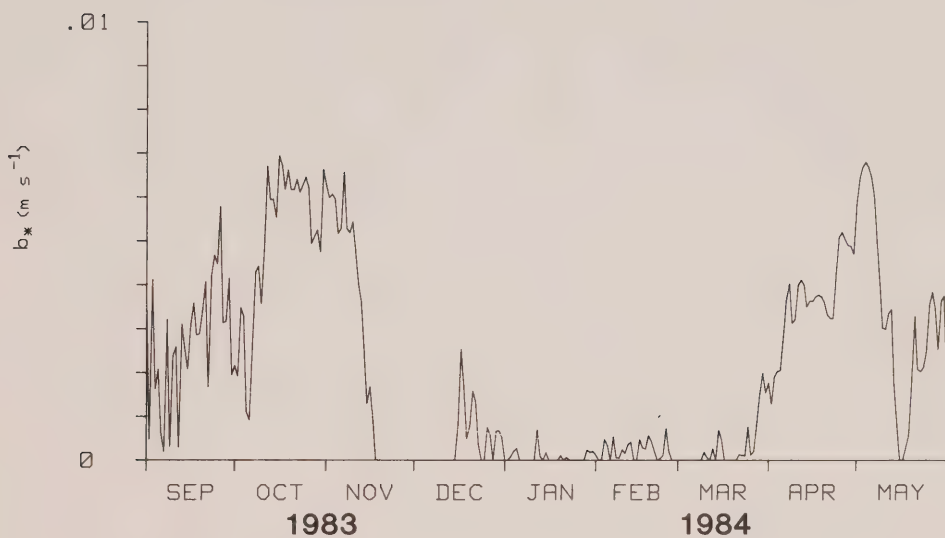


Figure C-2. The forcing parameter b_* (during convection) as a function of time.

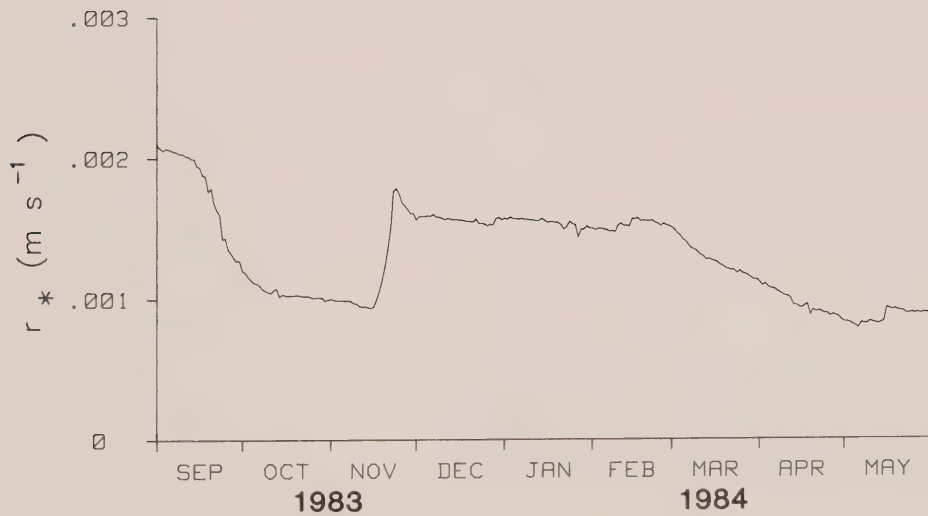


Figure C-3. The forcing parameter r_* as a function of time.

Appendix D
Seasonal Temperature Structure

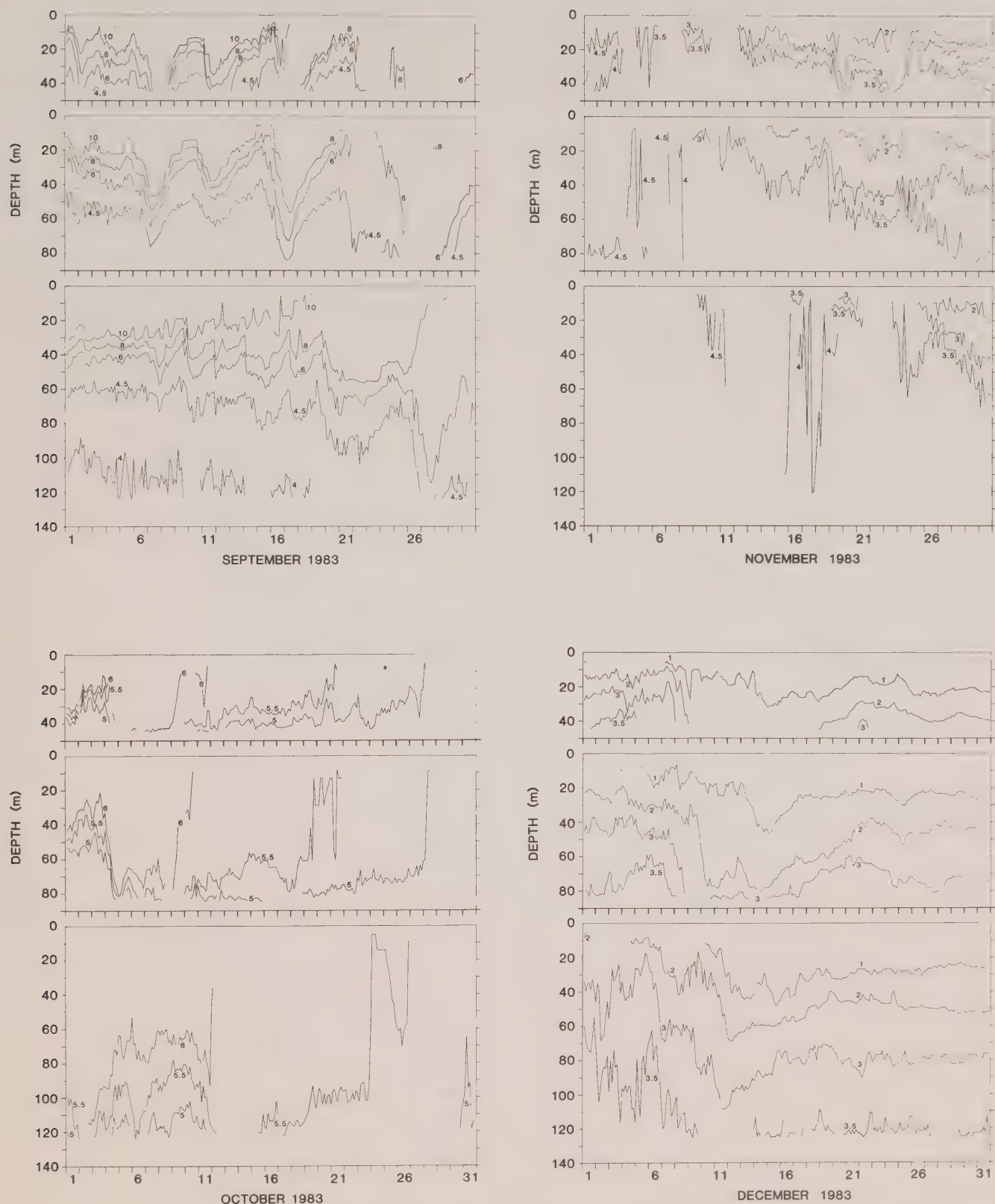


Figure D-1. Isotherm depth as a function of time at the three mooring sites.

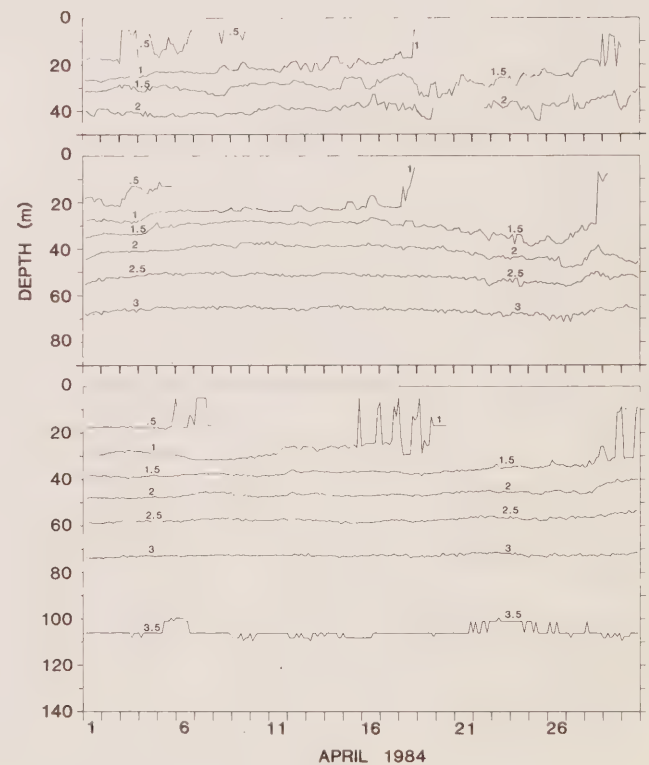
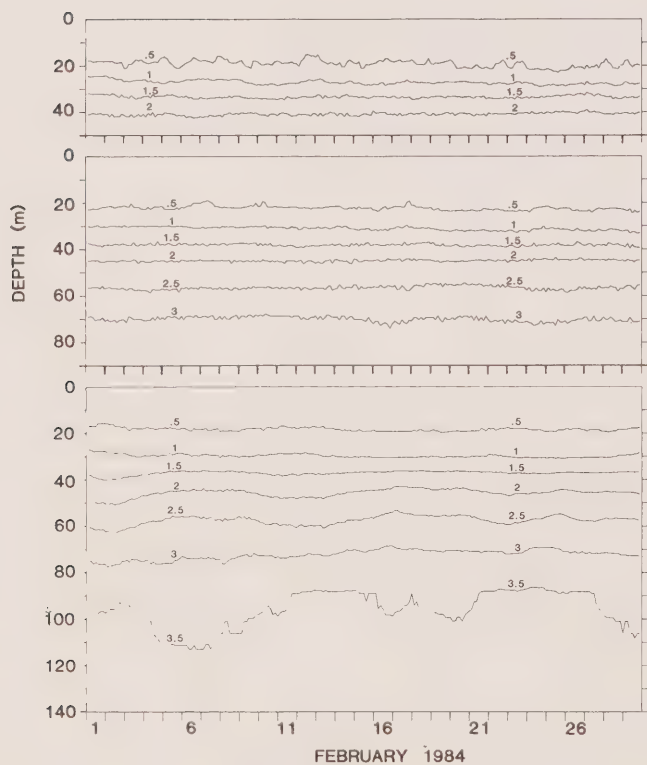
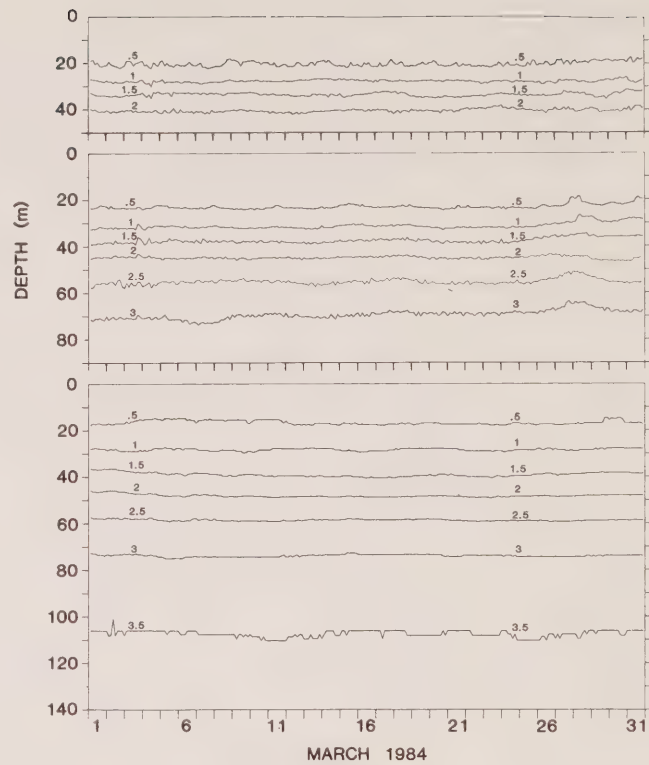
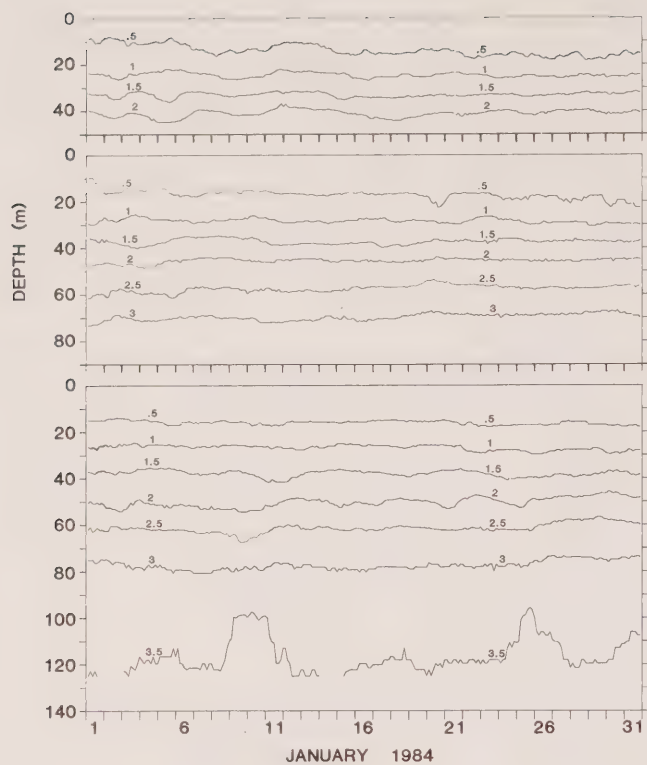


Figure D-1. Continued.

LAKE LABERGE

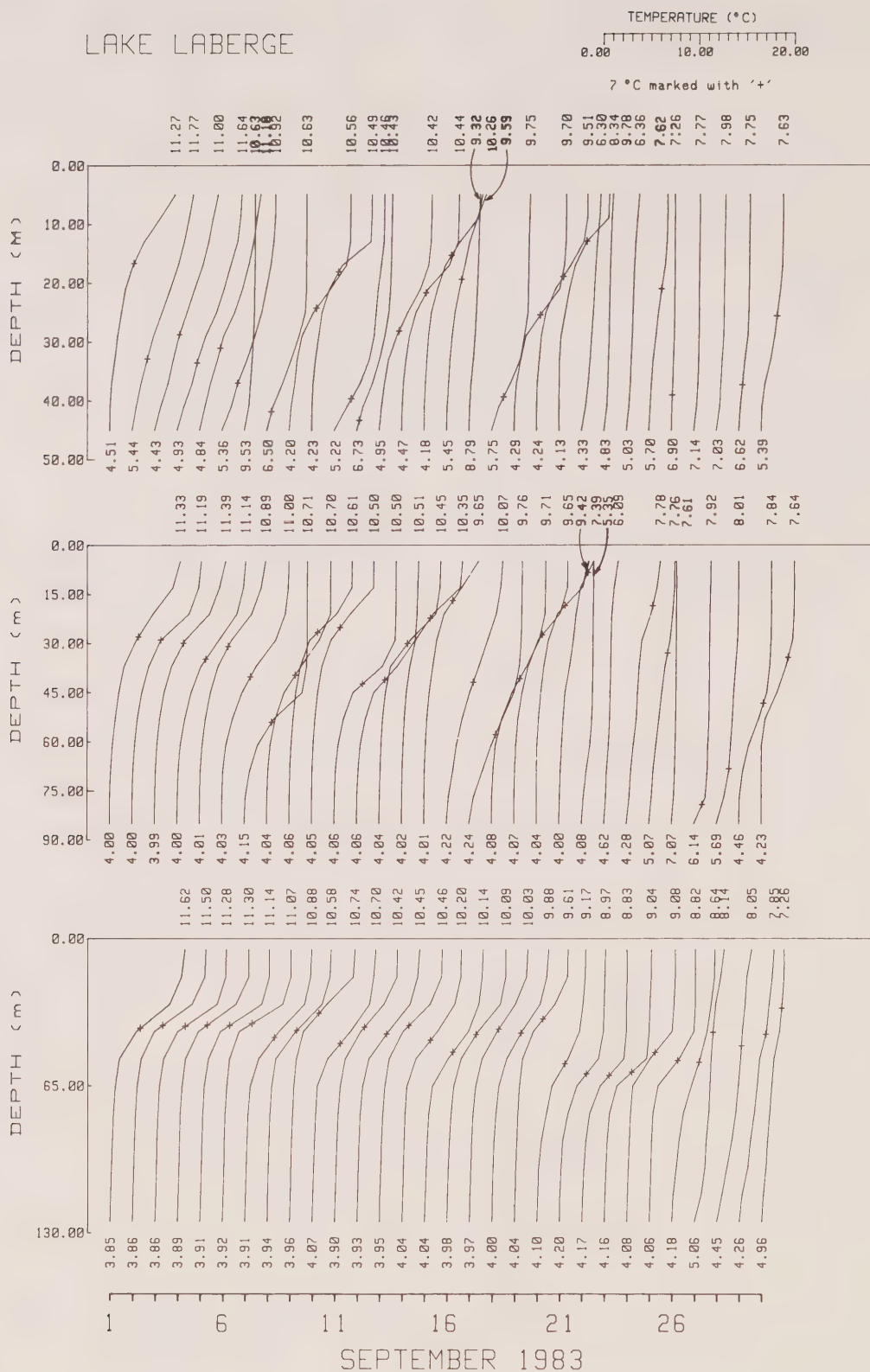


Figure D-2. Daily mean temperature profiles at the three mooring sites.

LAKE LABERGE

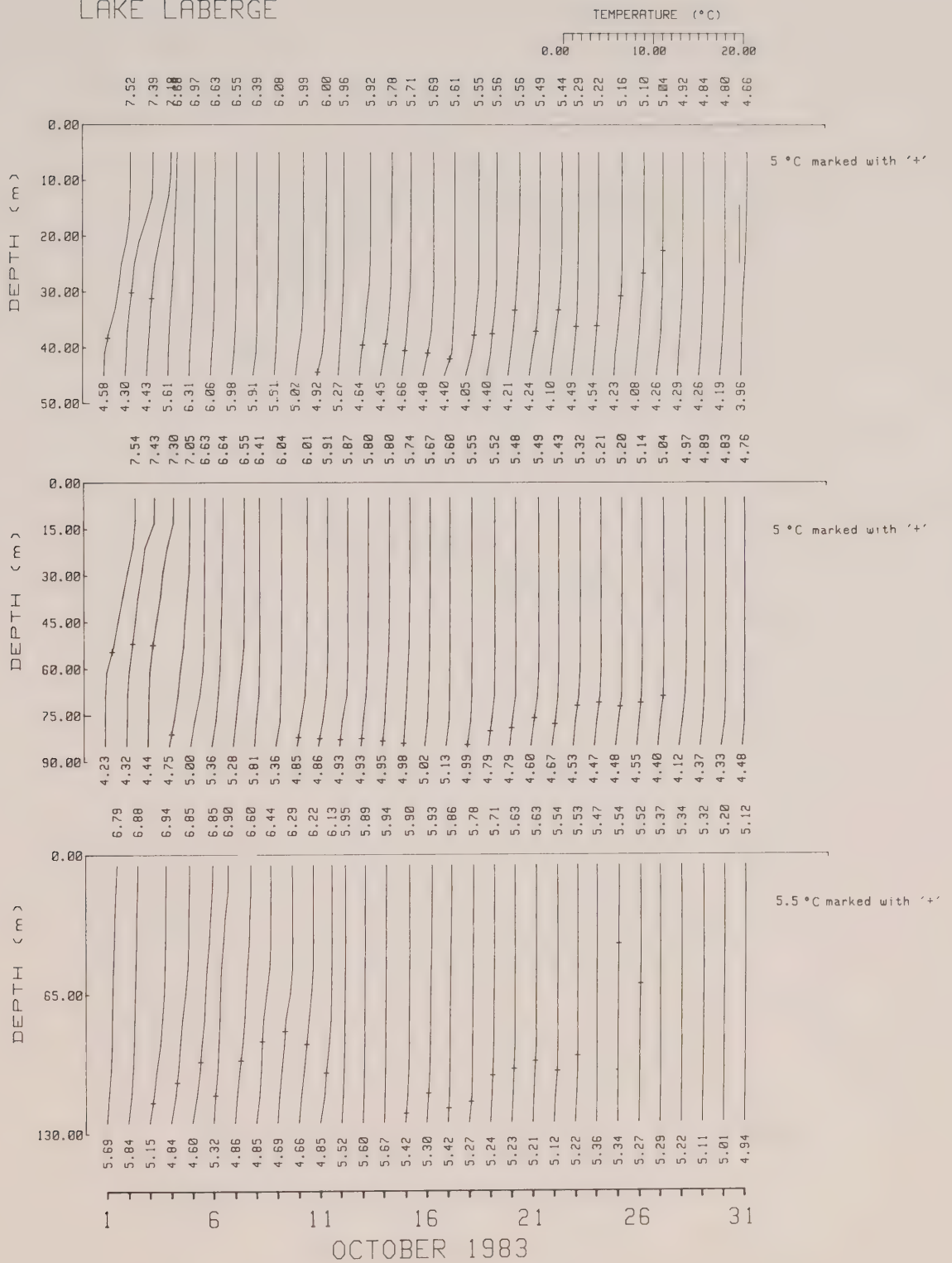


Figure D-2. Continued.

LAKE LABERGE

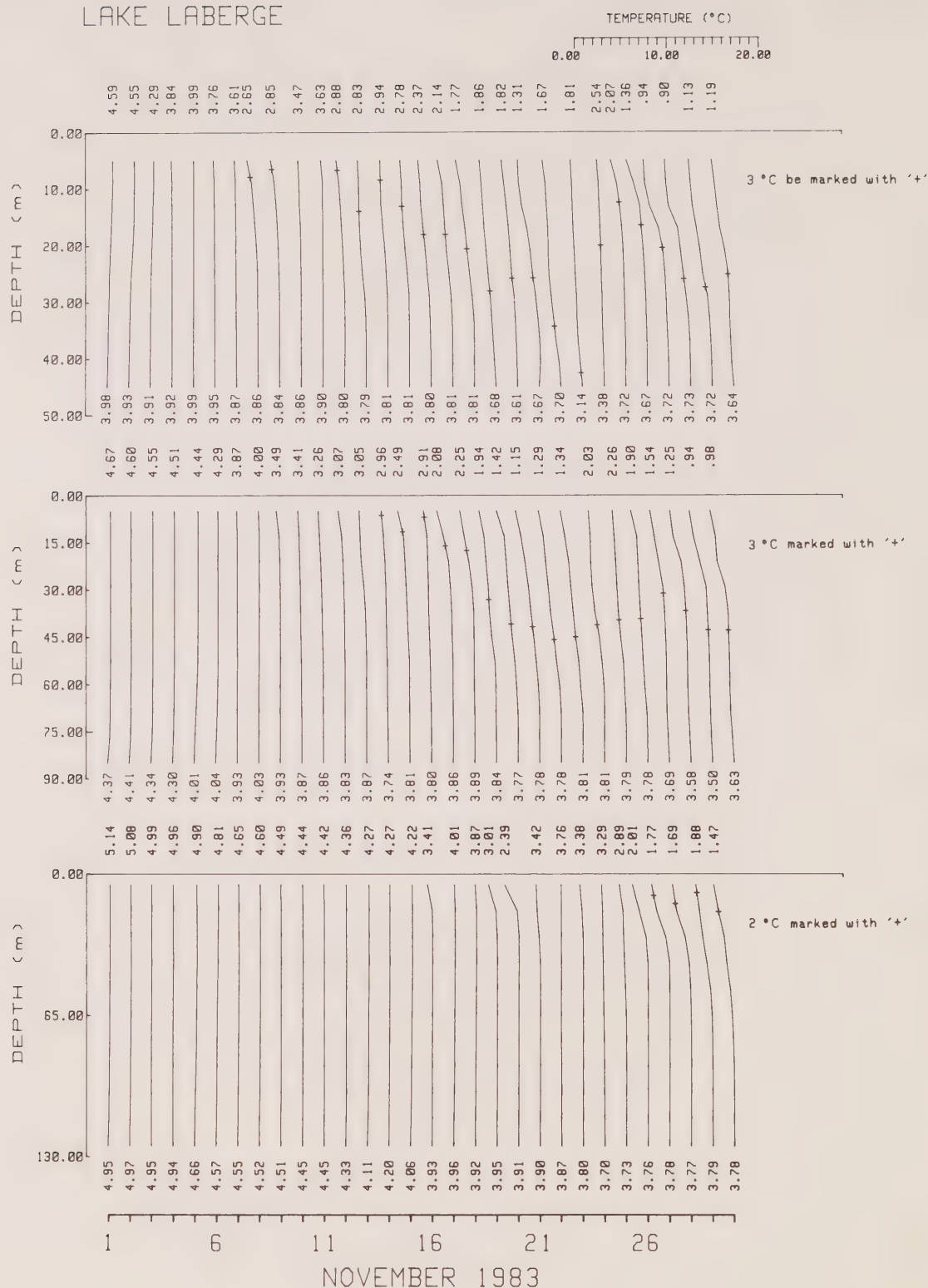


Figure D-2. Continued.

LAKE LABERGE

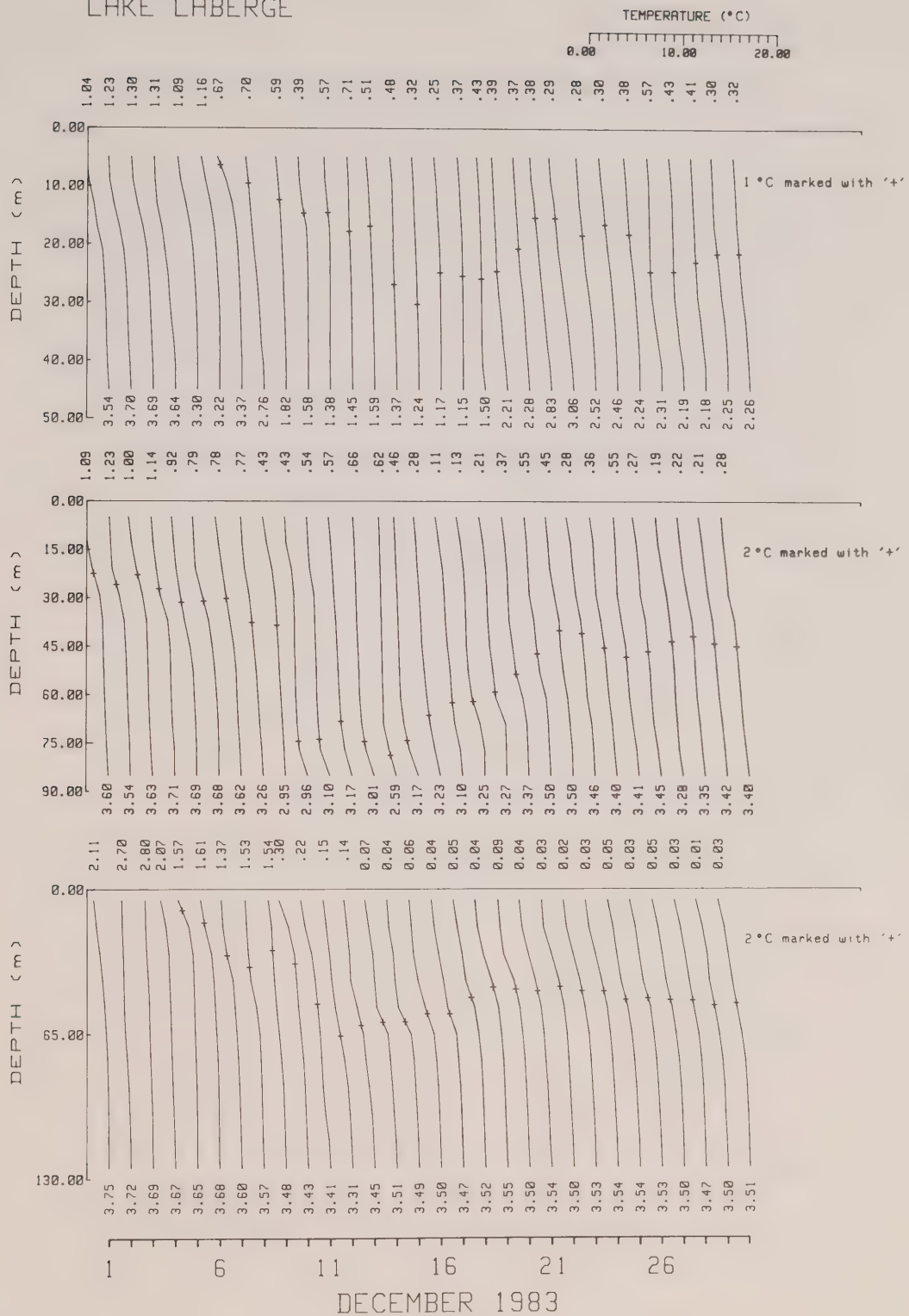


Figure D-2. Continued.

LAKE LABERGE

TEMPERATURE (°C):
0.00 10.00 20.00

2 °C marked with '+'

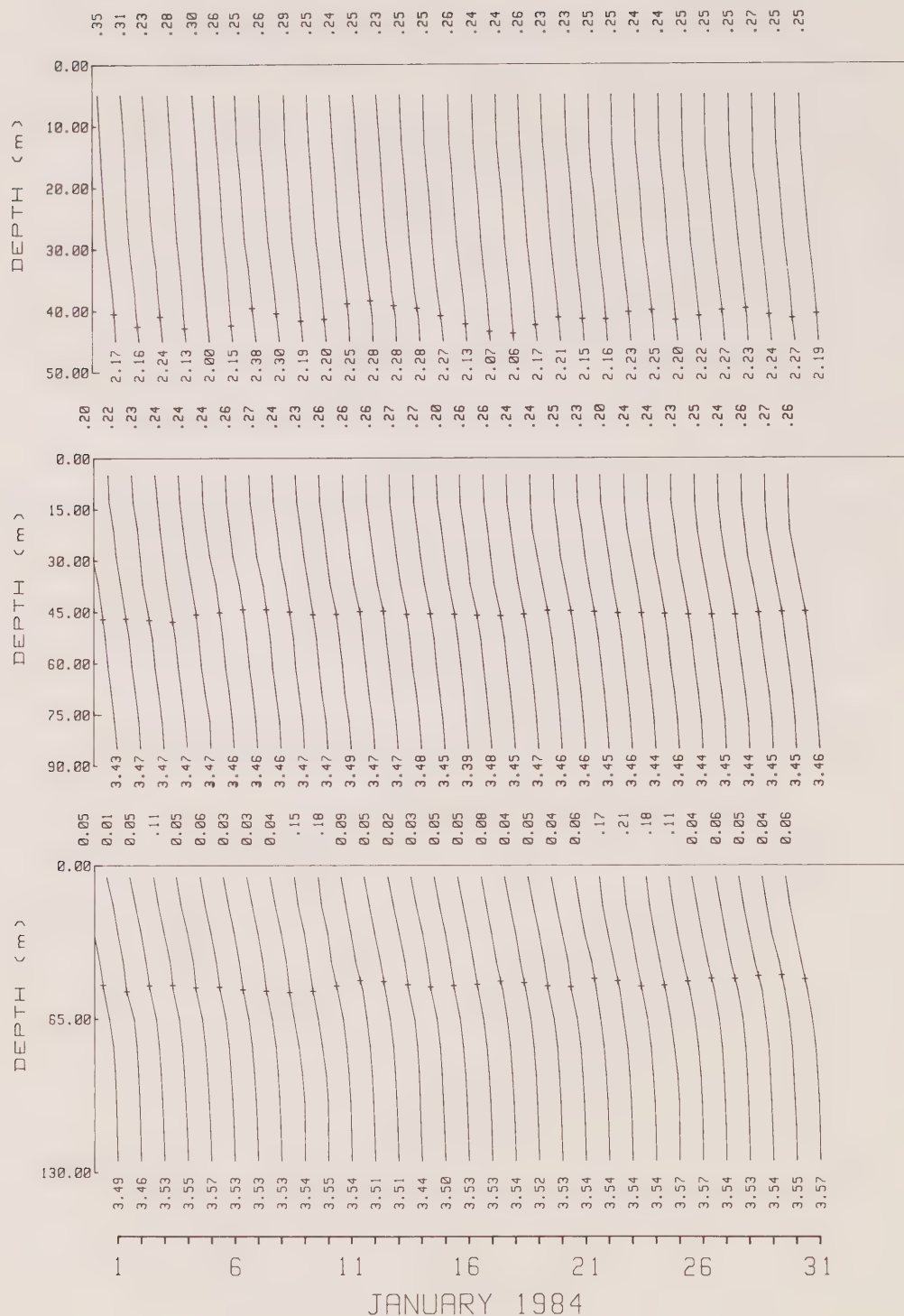


Figure D-2. Continued.

LAKE LABERGE

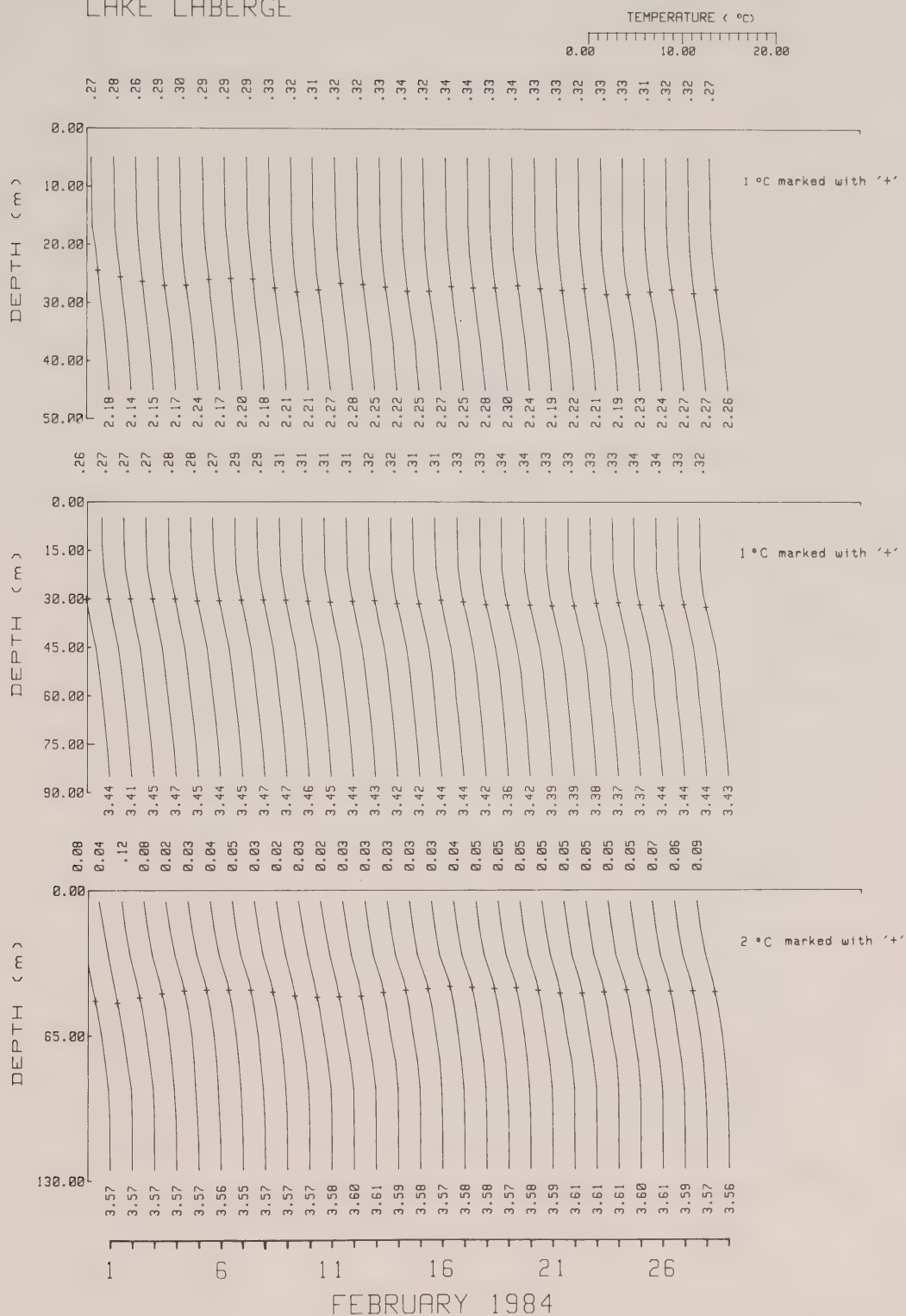


Figure D-2. Continued.

LAKE LABERGE

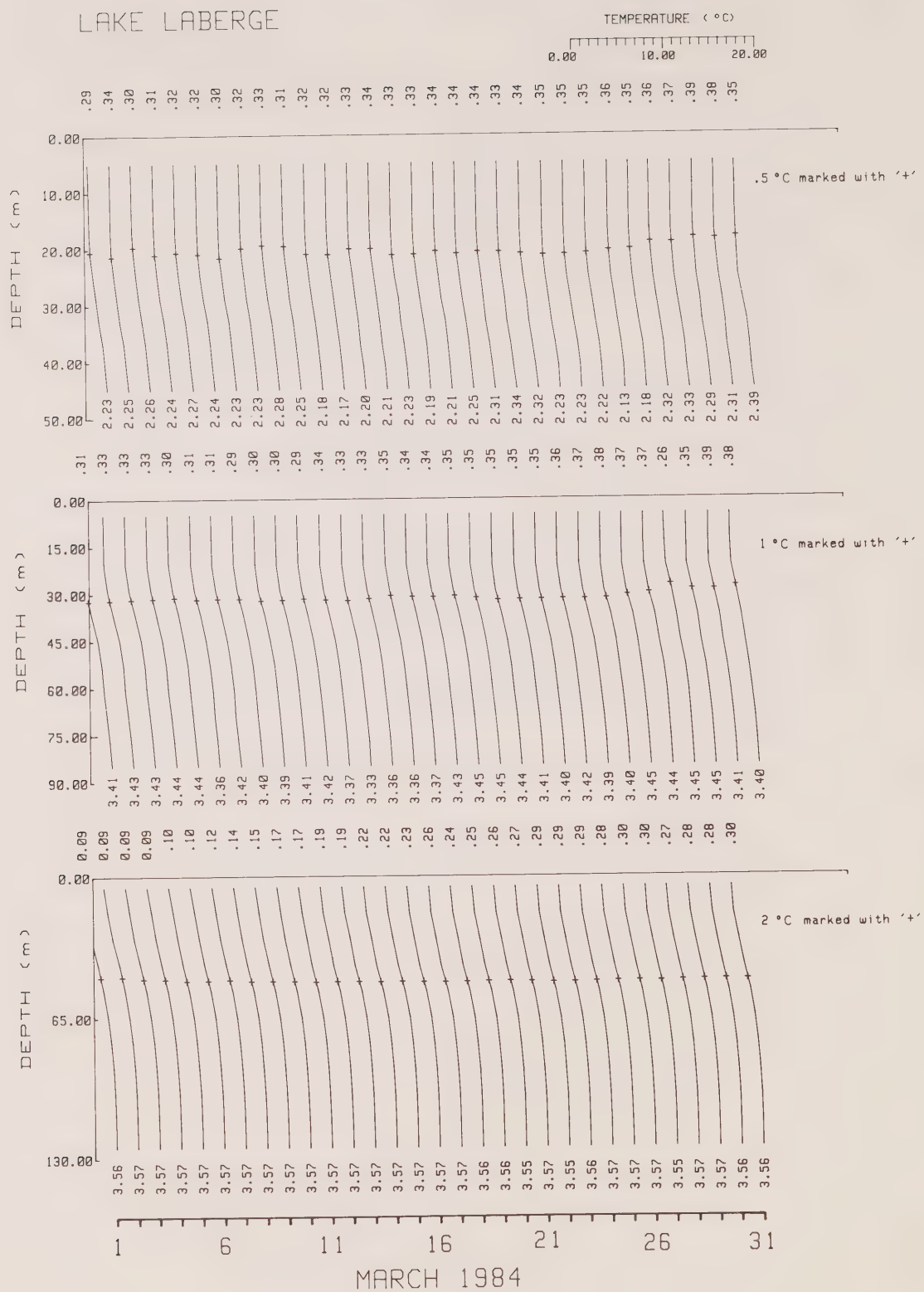


Figure D-2. Continued.

LAKE LABERGE

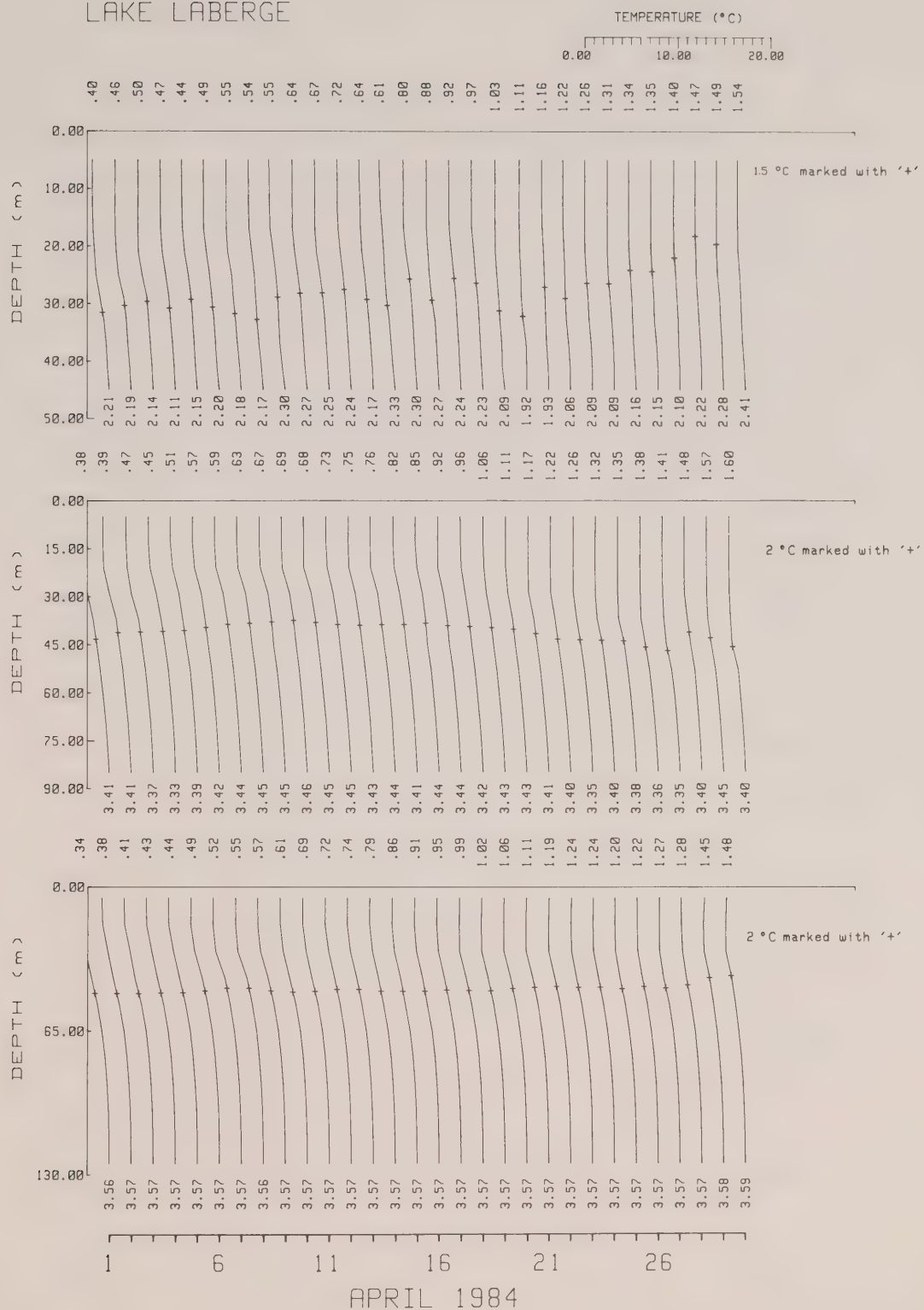


Figure D-2. Continued.

LAKE LABERGE

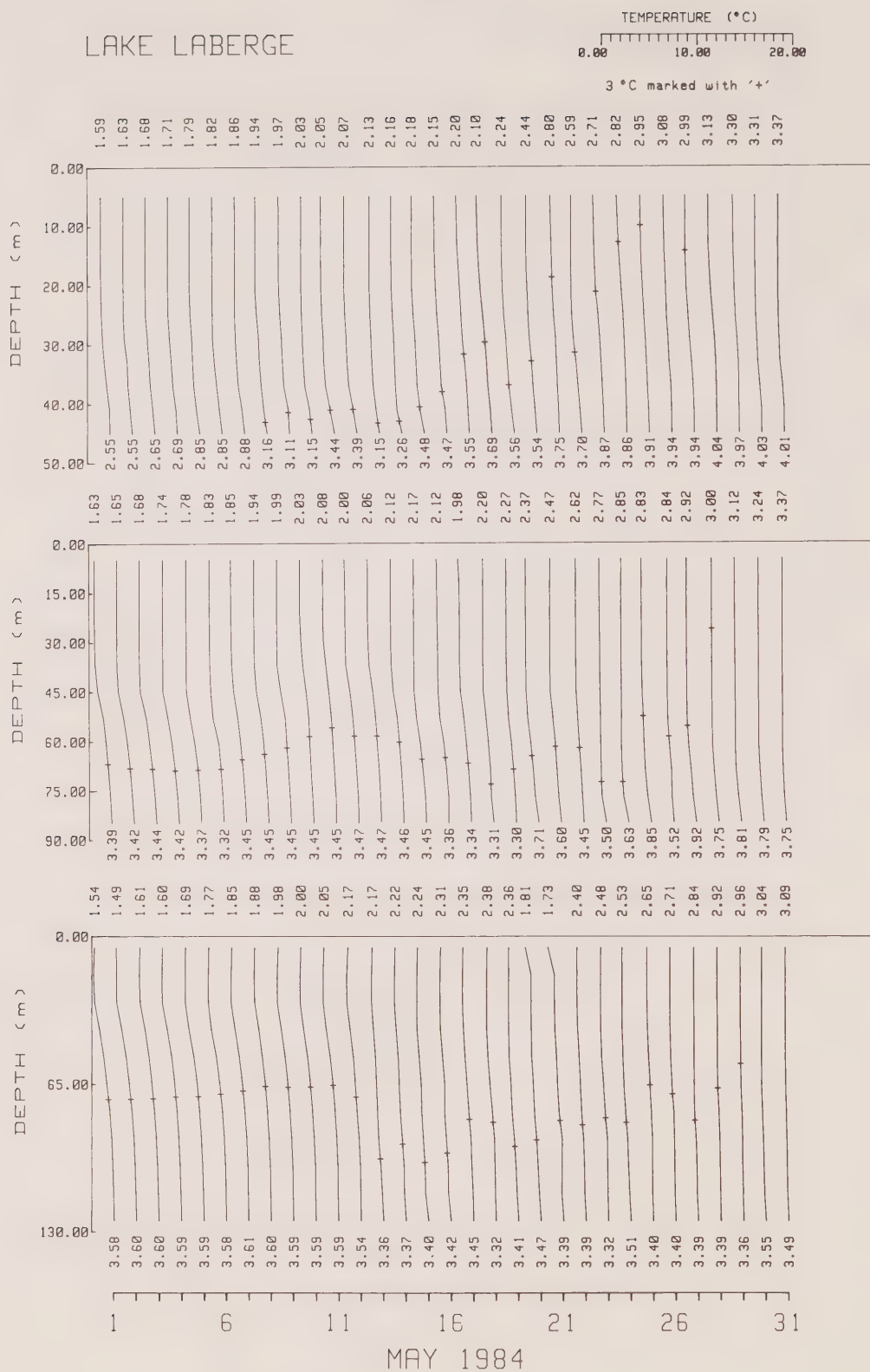


Figure D-2. Continued.

LAKE LABERGE

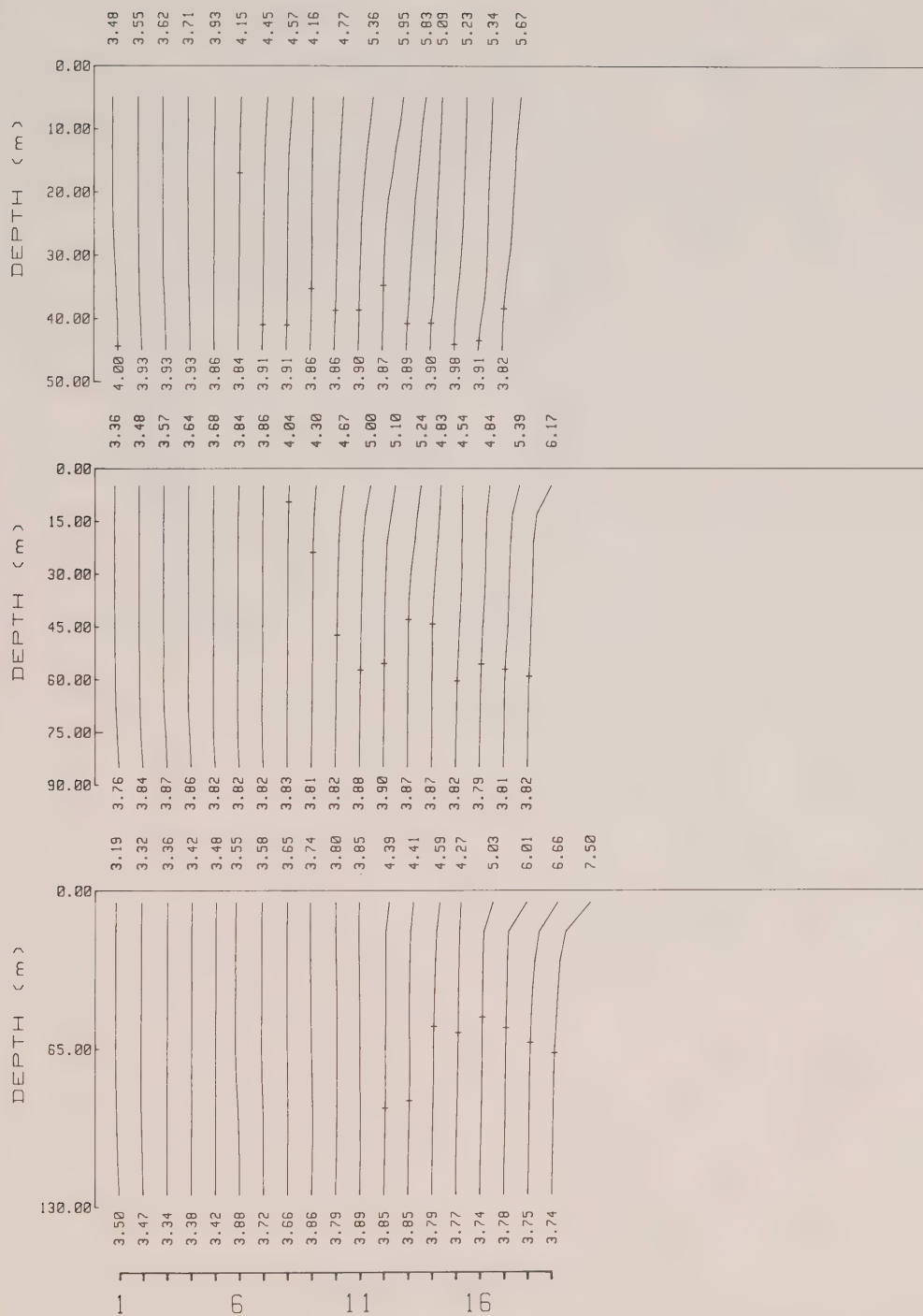
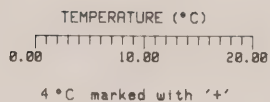


Figure D-2. Continued.

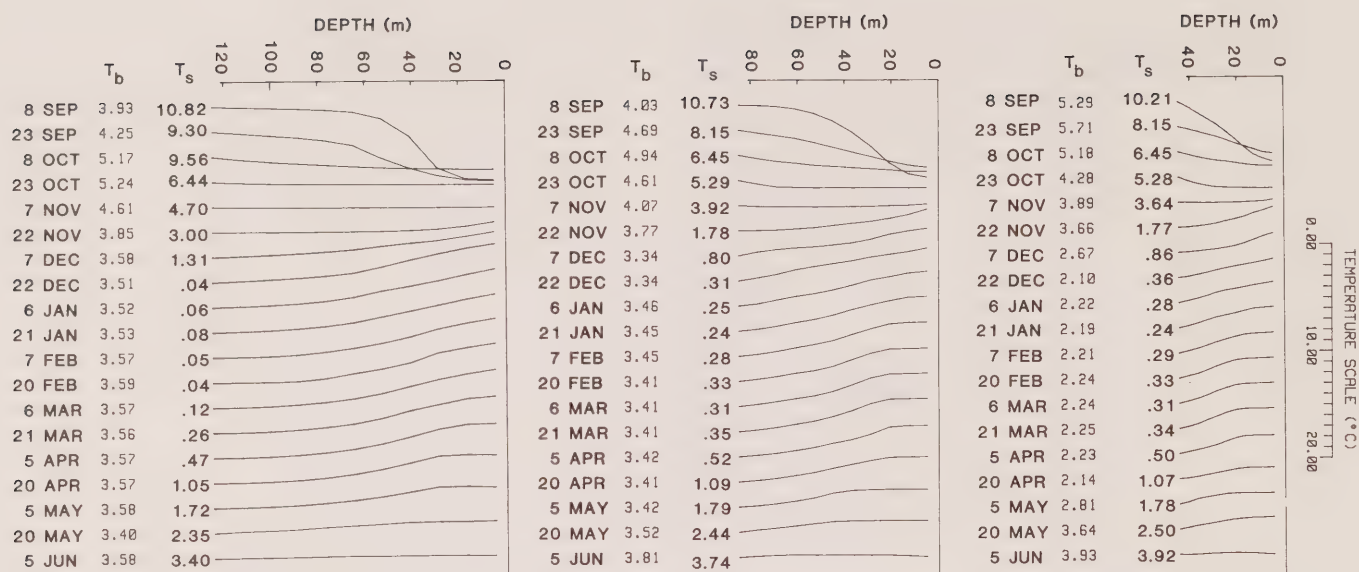


Figure D-3. Biomonthly mean temperature profiles at the three mooring sites.

Appendix E
Temperature and Conductivity Sections

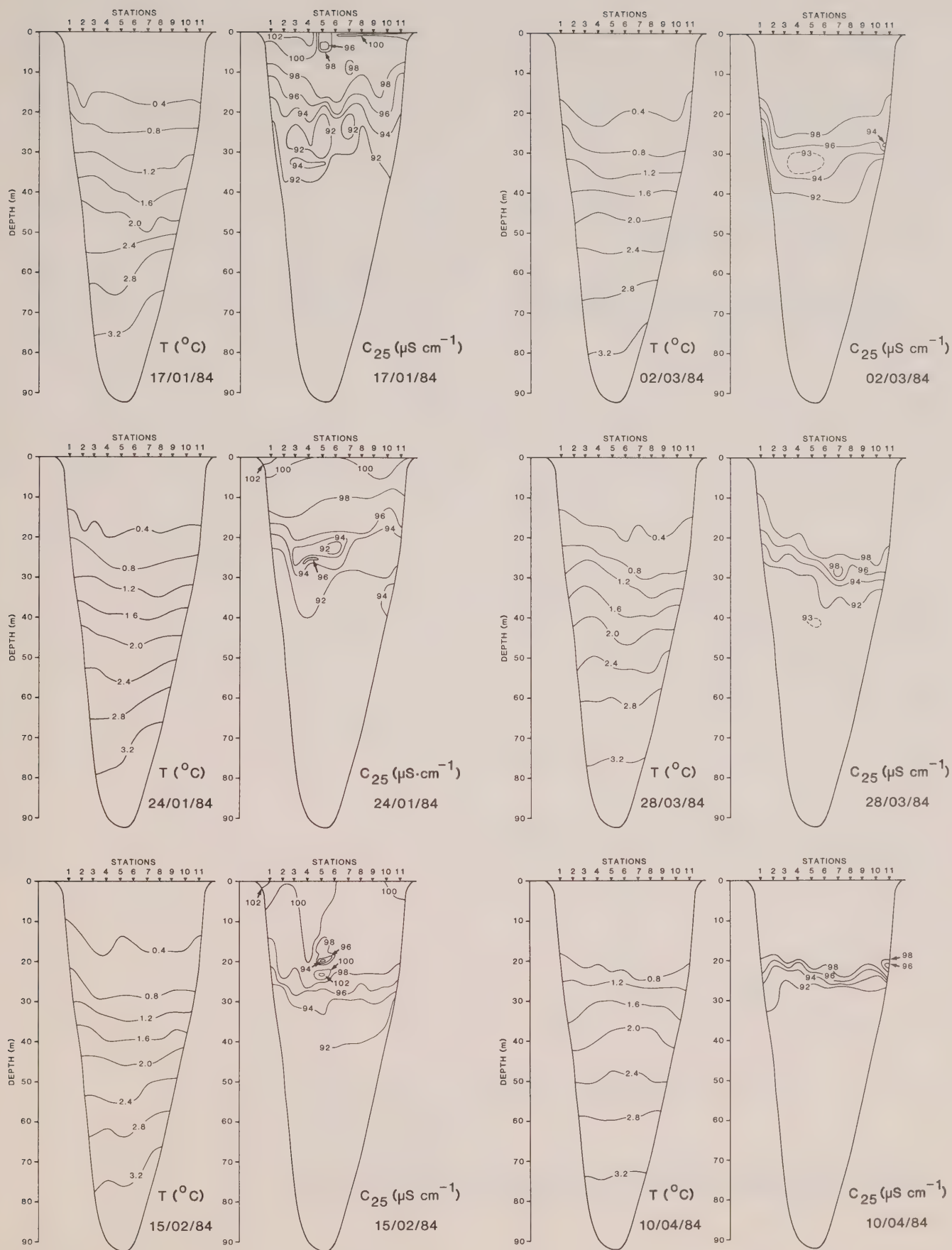


Figure E-1. Transverse sections of temperature (T) and conductivity relative to 25°C (C_{25}) at the Jackfish Bay section.

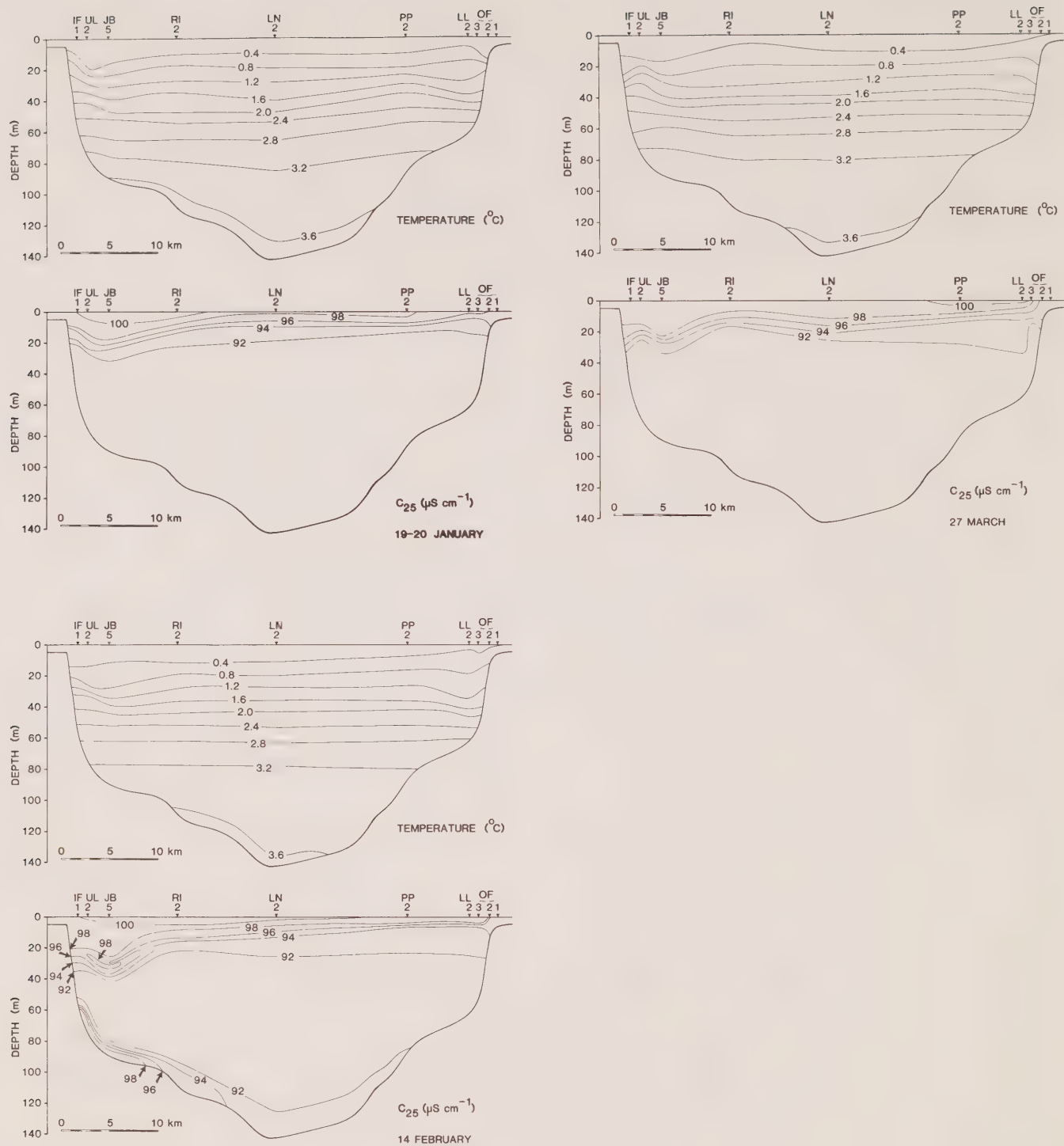


Figure E-2. Longitudinal sections of temperature (T) and conductivity relative to 25°C (C_{25}).

Appendix F
Horizontal Property and Distribution Maps



Figure F-1. Depth of the 0.5°C isotherm and C_{25} at the depth of the 0.5°C isotherm, January 17-20, 1984.



Figure F-3. Depth of the 0.5°C isotherm and C_{25} at the depth of the 0.5°C isotherm, March 27-28, 1984.



Figure F-2. Depth of the 0.5°C isotherm and C_{25} at the depth of the 0.5°C isotherm, February 14-15, 1984.



Figure F-4. Depth of the water mass boundary and $T^{\circ}\text{C}$ at the depth of the water mass boundary, January 17-20, 1984.



Figure F-5. Depth of the water mass boundary and $T^{\circ}\text{C}$ at the depth of the water mass boundary, February 14-15, 1984.

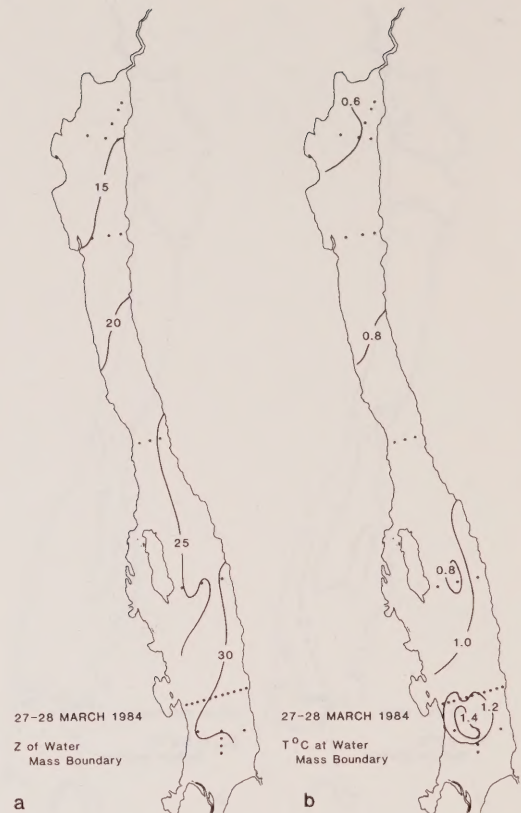


Figure F-6. Depth of the water mass boundary and $T^{\circ}\text{C}$ at the depth of the water mass boundary, March 27-28, 1984.

